Modeling Cell Migration Mechanics

9

Louis S. Prahl and David J. Odde

Abstract

Cell migration is the physical movement of cells and is responsible for the extensive cellular invasion and metastasis that occur in high-grade tumors. Motivated by decades of direct observation of cell migration via light microscopy, theoretical models have emerged to capture various aspects of the fundamental physical phenomena underlying cell migration. Yet, the motility mechanisms actually used by tumor cells during invasion are still poorly understood, as is the role of cellular interactions with the extracellular environment. In this chapter, we review key physical principles of cytoskeletal self-assembly and force generation, membrane tension, biological adhesion, hydrostatic and osmotic pressures, and their integration in mathematical models of cell migration. With the goal of modeling-driven cancer therapy, we provide examples to guide oncologists and physical scientists in developing next-generation models to predict disease progression and treatment.

Keywords

Mathematical modeling · Cell migration · Cell mechanics · Extracellular matrix

Abbreviations

ATP	Adenosine triphosphate
CMS	Cell migration simulator
ECM	Extracellular matrix
FEM	Finite element modeling
GBM	Glioblastoma (grade IV glioma)
ODE	Ordinary differential equations
PDE	Partial differential equations
RGD	Arginine-glycine-aspartic acid tripeptide
SDE	Stochastic differential equations
SSA	Stochastic simulation algorithm

9.1 Introduction: Cell Migration as a Physical Process

The remarkable physical process of cellular locomotion, termed migration, is one of the most extensively studied phenomena in biology. Throughout the organismal life cycle, cell migration plays key roles in directing biological processes from collective migration that shapes tissues during development, to

L. S. Prahl (✉) · D. J. Odde
Department of Biomedical Engineering and Physical Sciences-Oncology Center, University of Minnesota-Twin Cities, Minneapolis, MN, USA
e-mail: prahl025@umn.edu; oddex002@umn.edu

C. Dong et al. (eds.), *Biomechanics in Oncology*, Advances in Experimental Medicine and Biology 1092, https://doi.org/10.1007/978-3-319-95294-9_9

immune cell surveillance and repair mechanisms that maintain tissue integrity [1, 2]. On the darker side, pathological invasion and metastasis are hallmarks of high-grade, invasive tumors [3] highlighting a critical clinical need for rationally designed anti-motility therapies. Decades of studies, fueled by advances in molecular biology and light microscopy, have contributed to an extensive "parts list" of molecular components involved in migration, as well as rich physical descriptions of cellular mechanics. Despite the explosion of available experimental data, we still lack a comprehensive understanding of mechanisms that guide cell migration.

Abercrombie provided one of the first unified physical descriptions of cell migration, one he described as a cyclic process involving distinct and concurrently executed steps of front protrusion, adhesion, contraction, and rear detachment that lead to forward motion in a polarized cell [4]. These steps form the blueprint for mesenchymal migration best associated with fibroblasts on 2D flat substrates, which inspired seminal mathematical models of cell migration [5, 6]. Protrusion and contraction are largely driven by dynamic self-assembly and force-generating properties of the actin cytoskeleton and myosin motors. Cell surface adhesion receptors, such as integrins, recognize specific extracellular matrix (ECM) ligands and are capable of transmitting cytoskeletal contractile forces to surrounding tissue environments.

Subsequent works describe a striking plasticity of migration "modes" that can vary by cell type and tissue context [7], sometimes heightening or diminishing the role of specific molecular components. Amoeboid migration of certain immune and cancer cells can persist in the apparent absence of integrin-mediated adhesions [8, 9], possibly through frictional forces exerted on the extracellular environment [10, 11]. Osmotic pressure generated by aquaporins or ion pumps can drive motion for certain tumor cells within confined channels, even following addition of actin polymerization inhibitors that stall motion in other cell types [12]. Despite these apparent exceptions, most migration modes still fit into the general framework proposed by Abercrombie [4], coordinating protrusion that drives shape change with active force generation to drive motion relative to the substrate. Driven by an explosion of cutting-edge imaging techniques and sensitive measurements of cellular and molecular-scale forces [13], experimental efforts to dissect these alternative "modes" offer modelers a rich milieu of physical data for model development.

Extracellular environmental properties represent another challenge in understanding physiologically relevant cell migration mechanisms. Early cell migration studies were typically conducted on flat 2D plastic or glass substrates that are much stiffer than biological tissues. Pelham and Wang [14] introduced polyacrylamide gels (PAGs) as a simple approach to providing cells with a compliant substrate (Young's modulus ~0.1–100 kPa, consistent with biological tissues), now a widely used system because their surfaces can be functionalized with proteins to study ECM effects on cell migration. (Patho)physiological conditions in which cells migrate include myriad other factors not represented in these assays, such as aligned extracellular matrix fibers [15], shear forces from fluid flow [16], physically confined spaces between other cells [17], and other spatially and temporally varying physical and chemical cues [18]. In response to emerging techniques to image migrating cells in vivo [19, 20] or in vitro engineered environments that mimic tissue properties [20–22], models will need to adapt to incorporate and test these new conditions.

Ultimately, the grand challenge of modeling cell migration is to develop a general theoretical framework connecting experimental observations to physical laws that accurately capture underlying molecular details and environmental factors, across cell types, and in conditions of health and disease. The goals of this chapter are threefold: (1) to examine the basic physical principles underlying cell migration, (2) to review and critique existing models that incorporate these principles, and (3) to outline prospects for adopting cellular-scale modeling to predict cancer progression and treatment outcomes. The third point is of paramount importance in treat-

ing high-grade cancer, as tumor cell invasion and metastasis are the main cause of mortality in patients with malignant tumors. The goal of biophysical modeling in oncology should move toward accurately predicting patient outcomes and strive to guide rational design of treatments that target migration.

9.2 Protrusion, Adhesion, Contraction, and Beyond: Integrated Mechanical Steps of Cell Migration

Mathematical cell migration models have traditionally been built around the conceptual basis of coordinated steps of protrusion, adhesion, and contraction [4, 23]. However, the remarkable complexity and plasticity of cell migration have led modelers to diverse physics-based mathematical expressions for these individual steps. In this first section, we first separate the three canonical steps and discuss, individually, their mathematical implementation using existing models as examples. We then examine cases of whole-cell models that can successfully predict cell migration behaviors. Finally, we provide examples from a recently developed cell migration simulator (CMS) that can potentially relate to disease progression or predict therapeutic interventions in silico. While it is beyond the scope of this chapter to provide detailed analysis of each and every model, we aim to clearly and concisely elucidate these key principles to guide their implementation in physical oncology research and toward the clinic.

9.2.1 Protrusive Forces and Actin Self-Assembly

One of the most striking aspects of cell migration is cells' ability to adopt a wide range of shapes and to change direction or overcome obstacles by extending pseudopods. Existing models of cell migration have almost universally incorporated some protrusive mechanism, typically based on actin self-assembly [24], examples of which are shown in Fig. 9.1. Experimentally, dynamic actin is indispensible for most cell migration modes, with a few apparent exceptions [12]. Adenosine triphosphate (ATP) nucleotide hydrolysis by actin drives filament assembly, with new subunits primarily added at the "barbed" (+)-end (at rate k_{on}), while depolymerization (at rate k_{off}) mainly occurs at the "pointed" (−)-end (Fig. 9.1a). The first key step in the canonical model of fibroblast migration is polarization: the extension of a lamellipodium in the direction of forward motion, marking the front of the cell, while the nucleus and a smaller protrusion mark the rear [4]. Lamellipodium extension relies on the formation of a branched actin network (Fig. 9.1b), dependent on nucleation factors, such as the Arp2/3 complex [25, 26], which arranges barbed ends in the direction of protrusion, giving rise to a polarized network. Actin assembly pushes the plasma membrane forward to create a thin (100–200 nm) actin-rich sheet at the leading edge of the cell [27]. Membrane tension (μ) antagonizes and limits actin network expansion, providing an opposing force that moves actin filaments away from the leading edge and toward the cell body, termed retrograde flow. Actin filaments are disassembled by a variety of mechanisms (e.g., depolymerization, breaking, severing), creating new assembly-competent actin to fuel network assembly and further leading edge advance [24].

9.2.2 The Brownian Ratchet Model for Pushing by Cytoskeletal Filaments

How does actin polymerization push the lamellipodium forward? Individual actin filaments are the least rigid component of the cytoskeleton under compressive load ($\sim 10^{-26}$ N/m^2 compared with microtubule $\sim 10^{-23}$ N/m^2 bending rigidity [28]). At first glance, compliant filaments in direct contact with a rigid plasma membrane would be excluded from adding new actin monomers to their tips, precluding any sustained pushing force (Fig. 9.1a). Hill [29] originally proposed a Brownian ratchet model, where stochastic ther-

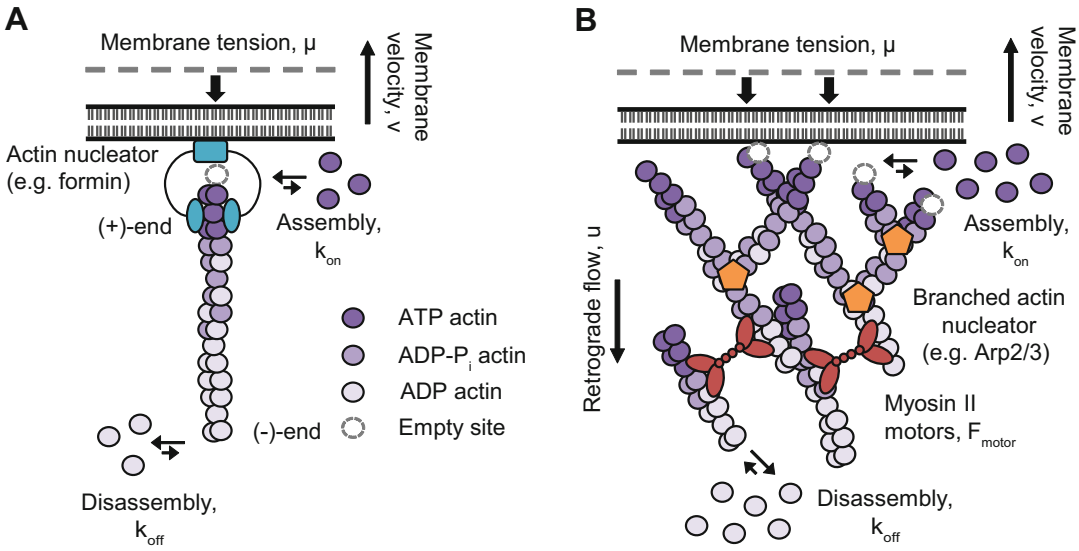

Fig. 9.1 Actin self-assembly and force-generating properties. (**a**) Force generation caused by a polymerizing actin filament against the plasma membrane (i.e., the "Brownian ratchet" model). Actin monomers (purple) exchange at both ends of the filament, but kinetic rates of assembly and disassembly (k_{on} and k_{off}, respectively, represented by arrows) are biased toward assembly at the "barbed" end (shown in contact with the plasma membrane, black) and toward disassembly at the distal "pointed" end. ATP hydrolysis occurs within the filament, distal to the tip, and is represented by changes in color within actin subunits. A dashed circle marks a possible new subunit addition site at near the plasma membrane, created by Brownian motion of the membrane and filament tip. Membrane tension (μ) provides an opposing compressive force on F-actin that resists polymerization. As new subunits are added, the plasma membrane is pushed forward at velocity (v), which depends on the membrane tension, association rate constant, G-actin concentration, and the size of actin monomers. Formins (cyan) create a "template" to catalyze this linear assembly in linear, actin-rich structures such as filopodia. (**b**) Branched actin networks, such as those nucleated by Arp2/3 complex in the lamellipodia of migrating cells, generate forward protrusion of the plasma membrane in a similar fashion. The branched structure allows the network to expand both forward and laterally, generating the sheet-like actin-rich structures. Opposing forces by membrane tension (μ) lead to retrograde flow of the actin network (u), frustrating forward protrusion of the membrane. Myosin II motors (red) cross-link actin filaments and hydrolyze ATP to slide filaments and facilitate network contraction. The total contractile force (F_{motor}) reflects the summed motor forces and can drive actin retrograde flow. Actin filament assembly and disassembly can also generate or relieve stress within the network, contributing to the total contractile force

mal fluctuations of the filament tip and plasma membrane can momentarily generate gaps for the addition of new monomers, essentially creating a drift in the membrane position. The Brownian ratchet theory was later elaborated to account for the filament architectures within cellular protrusions [30, 31]. Filament lengthening by subunit addition biases membrane diffusion in the direction of forward motion, which is powered by the favorable binding energy for subunit addition. The pushing force for an individual filament (f_0) thus depends on the free actin monomer concentration [M] and kinetic rates of assembly and disassembly, k_{on} and k_{off}, respectively.

$$f_0 = \frac{k_B T}{\delta} \ln\left(\frac{k_{on}[M]}{k_{off}}\right) \qquad (9.1)$$

In Eq. 9.1, k_B is Boltzmann's constant, so $k_B T = 4.18$ pNnm at $T = 310$ K. If each actin monomer added protrudes the membrane 2.7 nm, assuming a free actin concentration of 10 μM and equal binding and unbinding rates ($k_{on} = k_{off}$), Eq. 9.1 predicts a maximal pushing force of ~3.5 piconewtons (pN) per filament [30, 31]. Dickinson et al. [32] note that larger forces are potentially attainable via biased diffusion of a nucleotide state-dependent barbed end coupler. Cooperation between multiple filaments and "load

Actin polymerization pushing forces

sharing" ensures that at least some filaments do not exceed their stall forces and can still efficiently drive forward protrusion [27, 33]. Using these principles, the simple Brownian ratchet explains how filament assembly drives other cell protrusions, such as the long, parallel, cross-linked actin bundles that form filopodia [31, 34] or invadopodia that cancer cells use to penetrate dense basement membrane structures [35, 36].

9.2.3 Actin Dynamics and Turnover in Lamellipodial Protrusion

Keratocytes are a particularly well-studied model for cells migrating with a lamellipodium driven primarily by actin polymerization-based forces. Nearly constant leading edge extension rate across their broad lamellipodium simplifies analysis of steady-state actin assembly dynamics. In other cell types, asynchronous leading edge advance can result from the intermittent loading dynamics of adhesive substrate coupling [37, 38] (see Sects. 9.4.3, 9.4.4 and 9.4.5 for more details on modeling adhesions). Mathematical modeling of actin turnover within the keratocyte lamellipodium [33] illuminates a fundamental relationship between the numbers of actin ends involved in leading edge force production, membrane tension, and steady-state actin assembly and disassembly kinetics. Their ordinary differential equation (ODE) model found that protrusion rate has a biphasic dependence on filament number, meaning an intermediate number of force-producing filaments yields the fastest migration speed for a given membrane tension resistance. Cells having too few filaments generate insufficient pushing force, while having too many filaments depletes the available actin pool and stalls forward motion. Although their model does not explicitly consider substrate force transmission, it does quantitatively describe fundamental principles that generally apply to actin-based structures within in cell protrusions.

9.3 Contractile Forces and Cytoplasmic Flows

The actin cytoskeleton also generates contractile forces, which are the typical molecular source of the traction forces that motile cells generate on their environment. Actin filaments and myosin II motors form a dynamic, cross-linked, viscoelastic gel, while ATP consumption by these elements provides a driving force for gel compaction [39–41]. These types of actin gels, such as the actin layer that gives rigidity to the cortex, tend to have moduli in the ~kPa range [41, 42]. Dubbed "active gels," these systems are fundamentally out of thermodynamic equilibrium due to the conversion of chemical energy into mechanical force that can generate cytoplasmic flows within the cell [40, 43]. Actin filament depolymerization distal to the leading edge is sufficient to generate retrograde flow (Fig. 9.1b), although in most cell types myosin II motor forces are also involved in sustaining flows [44, 45]. Each actin filament [31, 46] or myosin II motor [47] can generate a few piconewtons (pN) of force, the net sum of which is the stall force (F_{stall}) of the cell. Estimates of $\sim 10^4$–10^5 myosin II motors per cell are consistent with maximum cellular outputs of 10–100 nanonewtons (n) for adherent cells [14, 48].

9.3.1 Actomyosin Force-Velocity Relationships

Actin flows are a highly conserved feature between different organisms and cell types and between the various "modes" of migration [49]. For well-adherent mesenchymal cells, actin retrograde flows can establish significant ($\sim 10^2$–10^3 Pa) traction stresses on the extracellular environment [44, 50]. The specific properties of adhesions and mathematical models for their behavior are described in greater detail later in this chapter (Sect. 9.4). Even in the absence of

specific adhesion complexes (characteristic of amoeboid migration), cortical actin flows can generate non-specific frictional forces on the extracellular environment to drive motion [10, 51]. Simultaneous measurements of traction and F-actin flow in cells demonstrate a clear inverse relationship between the two [37, 50, 52], which is explicitly assumed by some models of traction force generation [37]. A typical expression is based on the original Hill equation for contraction of a muscle under tension [53], Eq. 9.2.

$$v = v_{\text{motor}} \left(1 - \frac{F_{\text{sub}}}{n_{\text{motor}} F_{\text{motor}}} \right) \tag{9.2}$$

In Eq. 9.2, the force transmitted to the substrate (F_{sub}) opposes the total cell stall force, here contributed by n_{motor} individual myosin II motors, each generating F_{motor} stall force [47]. This slows flow from its maximal velocity (v_{motor}), typically ~100 nm/s for both actin polymerization and myosin II motors sliding filament actin bundles [30, 54]. This relationship assumes the actin filaments and myosin motors are rigid, a reasonable assumption for individual actin filaments given tensile strength measurements in the hundreds of pN [55]. Force-velocity relationships have been experimentally observed for both actin polymerization [30, 32] and myosin II motors working against an opposing load [54, 56, 57].

9.3.2 Actin Flows Antagonize Protrusion to Produce Cell Shapes

A combination of actin polymerization and actin flows are sufficient to drive large-scale rearrangement of cell shape, leading to polarized migration. Returning to the highly motile keratocyte model system, Barnhart et al. [58] developed a moveable cell boundary model using partial differential equations (PDE) where the velocities of points along the cell outline are determined by the difference between actin protrusion and retrograde flow. If protrusion is faster than retrograde flow at a given point, the cell will elongate in that direction, while if the reverse is true, retraction occurs. Interestingly, and consistent with their experimental measurements, the ability of a cell to establish polarity depended on the degree of adhesion to the substrate, here modeled as frictional drag on the surface for a variable density of adhesion sites. At low adhesion levels, cells were round and contained fast flowing actin. Flows were drastically slower when adhesion levels were high, and cells stalled on the adhesive surface. At intermediate adhesion levels, polarity and migration recovered, demonstrating that establishment of stable cell protrusions requires a balance between polymerization and flow, with adhesion serving as a coupler between them. In a similar fashion, highly contractile epithelial cells, which are typically nonpolar and immobile, can undergo spontaneous symmetry breaking upon inhibition of myosin II [59]. In these cells, myosin II immobilizes actin in circumferential bundles around the cell and suppresses spontaneous polarization. Relaxing the bundles by inhibiting myosin II frees actin to self-assemble into protrusive networks and establishes polarity and movement, consistent with a model requiring a balance between contractile forces and protrusion. Other models, such as by Satulovsky et al. [60], generate simulated cells that protrude and retract in response to locally excitable protrusion (i.e., actin polymerization) and global retraction signals (i.e., retrograde flow). Although their model does not incorporate any mechanism of direct force generation, it shows that these competing signals can drive a wide range of cell shape changes, including the disparate morphologies of keratocytes and neurons, with a limited number of parameters. Thus, actin flows and their relation to actin assembly and protrusive forces emerge with key functions in shaping cells and guiding migration.

9.3.3 Actin Flows Reinforce Polarity in Persistent Migration

Robust actin flows also establish persistent fast migration in highly polarized amoeboid cells [51, 61, 62]. Maiuri et al. [61] identified a power law relationship between actin flow speed and protrusion lifetime, which was consistent between a wide array of cell types and environments. Their diffusion-convection-reaction model quantitatively predicts intracellular gradients of actin-binding factors (such as myosin II) that are established by actin retrograde flows and illustrates a close relationship between polarity and migration. Actin flows emerge as a major determinant of protrusion lifetime (τ), which enables a switch between slow "random" and fast "persistent" trajectories, as well as an "intermediate" phenotype that stochastically switches between the two. Although the Maiuri et al. model replicates an important relationship involved in determining cell migration behaviors, and can replicate both in vitro and in vivo cell tracking results with only two tunable parameters (the actin flow speed and polarity factor concentration), it does not consider force transmission to the substrate, an important determinant of cells' ability to sense environmental stiffness (Sect. 9.4).

Poorly adhesive environments with a high degree of mechanical confinement promote spontaneous polarization and fast migration in a manner that depends on myosin II activity [51]. This is thought to be due to fluctuations in binding and unbinding of myosin II to cortical actin, which may weaken the cortex and lead to the establishment of large bleb or membrane distension [63] driven by intracellular pressure (Sect. 9.5). Spontaneous polarization in this so-called "leader bleb" migration was also likelier for certain immune cells and transformed cells, compared to their healthy counterparts [51], suggesting a conserved motility mode that may be activated by high myosin II activity under certain tumor conditions. Ruprecht et al. [62] similarly demonstrated that high myosin II activity and anisotropic tension within the cortex are sufficient to initiate and maintain polarization in zebra fish germ line cells, suggesting this phenotype may also occur for cells in specific stages of development.

9.4 Adhesive Bonds and Force Transmission to the Substrate

Force transmission to the ECM is the final step in the canonical model of cell migration. Many migrating cells transmit actomyosin forces to the substrate through adhesion receptors that recognize and reversibly bind specific ECM components [64, 65]. Cells express a wide variety of adhesion receptors, such as integrins, cadherins, and other membrane-spanning molecules such as CD44, each of which bind to specific ECM ligands or other cells [65–68]. Adhesion receptors are key components for their roles in coupling actin dynamics that control protrusion (Sect. 9.2) and contraction (Sect. 9.3) to motion via traction forces on the substrate (Fig. 9.2a). Traction stress and strain energy output may also depend on cell size and geometry, which is captured by continuum models that forego modeling individual adhesion dynamics [70]. Because ECM composition and cell adhesion receptor expression may change in cancer [71], we now focus on principles of molecular-scale adhesion dynamics that enable cells to tune their responses to environmental mechanical and chemical factors.

Integrin-containing focal adhesions are by far the best-characterized type of adhesion complexes formed by adherent cells and contain well over 100 distinct proteins involved in signaling and force transmission [72]. Integrins are transmembrane proteins that form $\alpha\beta$ heterodimers, each of which recognizes a specific extracellular matrix ligand; in humans, there are 18 α isoforms and 8 β isoforms with many functionally redundant combinations that bind similar ligands [64]. Integrin intracellular domains engage actin filaments through adaptor proteins such as talin, α-actinin, and vinculin, enabling transmission of actomyosin-based forces to the extracellular environment [65, 73, 74].

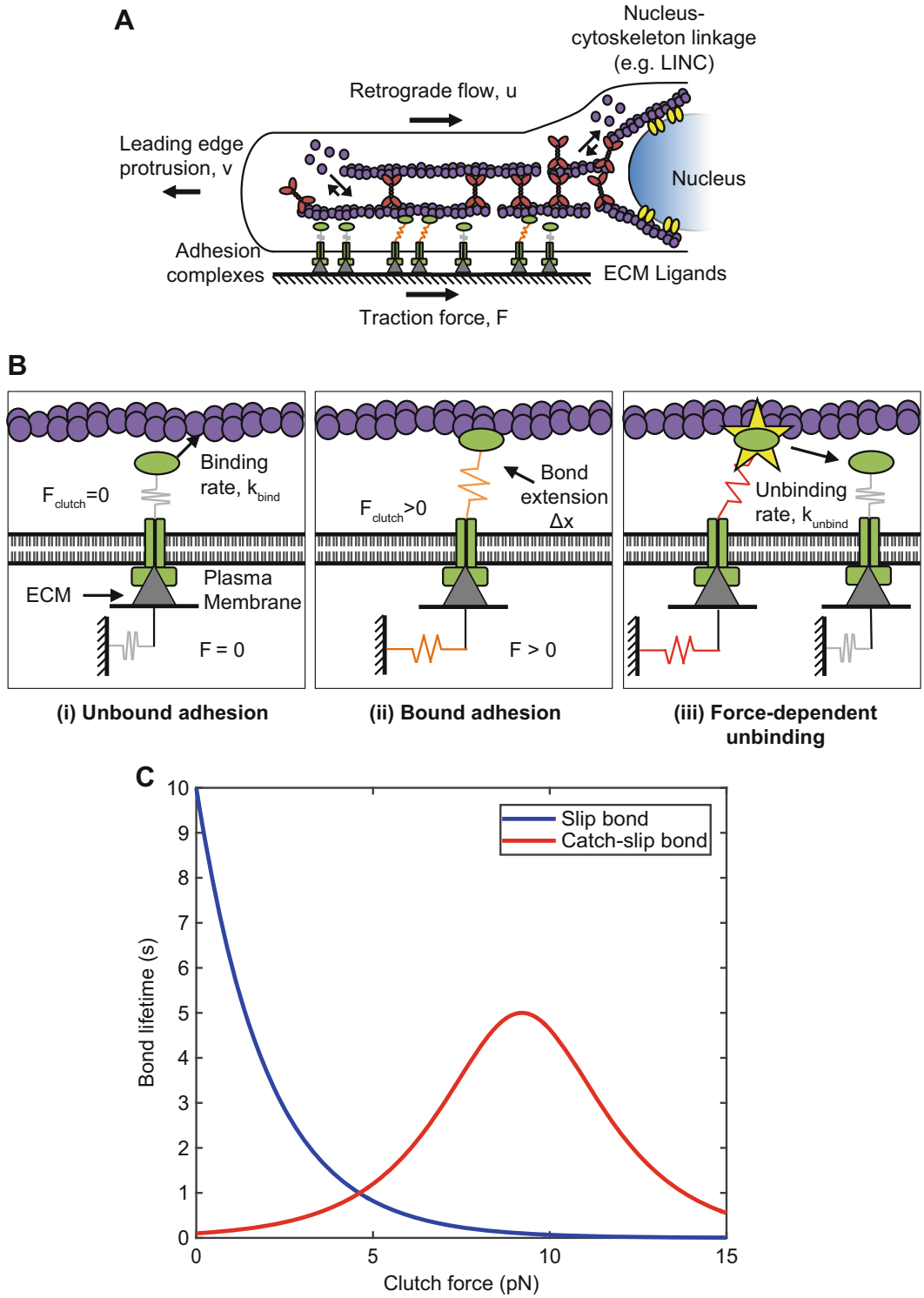

Fig. 9.2 Principles of cellular adhesion and force transmission. (**a**) Schematic of the mechanics of actomyosin-based force generation and transmission within a cellular protrusion. F-actin polymerization against the membrane drives forward protrusion of the leading edge at velocity, v_{edge}. Forces from membrane tension and contraction of

For different adhesion receptors, such as CD44, the adaptor protein role of talin and vinculin in linking to the cytoskeleton may involve other molecular players such as ezrin/radixin/moesin (ERM) proteins [68]. Bonds formed between the ECM, integrins, adaptors, and actin filaments are highly dynamic (Fig. 9.2b), and the kinetics of bond association and dissociation are strongly force-dependent [18]. Notably, different integrins may bind their ligands with different kinetics, which can affect traction force outputs in environments of varying stiffness [75]. This stiffness sensing by dynamic adhesions regulates important biological functions, such as stem cell differentiation [76], tumor cell proliferation [77], transcription factor nuclear localization [78], and, this chapter's primary focus, cell migration [79].

9.4.1 Slip Bonds

To a first approximation, the binding rate between adaptor proteins and actin filaments (alternatively, adhesion receptors and their ECM ligands) can be considered first-order reactions, since they are in close proximity within the focal adhesion complex or the cell-substrate interface. Unbinding events occur with increasing frequency as actin retrograde flow builds forces on individual bonds. Early models of cell adhesion [69] refer to a so-called "slip bond" behavior (Fig. 9.2c) in which the force on a particular bond (F) scales a basal off-rate for the slip bond ($k_{\text{off,s}}$).

$$k_{\text{off}} = k_{\text{off},s} e^{\left(F / F_{\text{bond},s}\right)} \tag{9.3}$$

Equation 9.3 predicts that the slip bond dissociation frequency increases with increasing load, while the property $F_{\text{bond,s}}$ is the characteristic scaling force for the slip bond. Slip bonds provide a straightforward example of force-bearing linkages that dissociate under a few pN of load, such as the bond between fibronectin and $\alpha_v\beta_3$ integrin [80].

9.4.2 Catch-Slip Bonds

Other bonds exhibit "catch-slip bond" behavior, where longest lifetimes occur at an intermediate force (Fig. 9.2c). The "catch" term refers to the weak association between a receptor and its ligand at low force, which strengthens as force increases. At higher forces, the bond functions as a slip bond, and detachment becomes more likely with increasing force. Integrins [75, 78, 81], the cadherin-catenin complex [82], and other types of adhesion molecules [83, 84] display catch-slip bond behavior under certain conditions. Bond lifetimes measured in vitro between

Fig. 9.2 (continued) the F-actin network by myosin II motors drive retrograde flow of F-actin inward, toward the cell nucleus, where nucleus-cytoskeleton linking complexes (yellow) provide mechanical continuity within the cell to allow connection to other protrusions (not shown). Distal to the leading edge, F-actin network disassembly occurs as described in Fig. 9.1b. Adhesion complexes (molecular clutches) are transmembrane structures (green), which transiently bind both F-actin and the ECM and can transmit traction forces on the extracellular matrix through their extension (orange springs) by retrograde flow. Adhesions that are not bound to actin (gray springs) do not contribute to the traction force. Adhesions are considered molecular "clutches" (**b**), which undergo force-dependent cycles of binding and unbinding. An unbound adhesion (i) is shown disconnected from the F-actin bundle but bound to the ECM. When unbound, force on the clutch (F_{clutch}) and traction force on the substrate ($F_{\text{substrate}}$, gray spring) are both zero. When the clutch binds at rate k_{bind}, (ii) retrograde flow (v_{flow}) extends the bound clutch (Δx), increasing the force on the clutch and force transmitted to the substrate. As force builds (iii), clutch unbinding (k_{unbind}) becomes increasingly likely, relaxing the load on the clutch and substrate. For an ensemble of clutches, as in an adhesion complex, cooperative behaviors may arise to increase the total force and effective bond lifetime of force transmission. (**c**) Molecular clutch binding lifetimes may follow any of several force-dependent behaviors: for "slip bonds" (blue line), unbinding becomes exponentially more likely with increasing load (a.k.a. Bell's law [69]), while for "catch-slip bonds" (red line), peak lifetimes occur at an intermediate force, while detachment is faster for lower or higher forces. Slip bonds and catch-slip bonds were modeled using Eqs. 9.3 and 9.4, respectively

$\alpha_5\beta_1$-integrin and fibronectin-binding domain peak at applied loads of 20–30 pN [81], easily within range of the forces observed at individual focal adhesions using molecular tension sensors [85, 86]. Catch-slip bond dissociation rates are typically modeled using a two-exponential model (Eq. 9.4) that includes the slip bond behavior (Eq. 9.3), plus an additional off-rate constant ($k_{\text{off,c}}$) and bond force ($F_{\text{bond,c}}$) for the catch behavior.

$$k_{\text{off}} = k_{\text{off},\ s} e^{\left(F / F_{\text{bond},s}\right)} + k_{\text{off},\ c} e^{\left(-F / F_{\text{bond},c}\right)} \tag{9.4}$$

Other models that describe more detailed multistep kinetic models defined by transition probabilities between different bound states are discussed elsewhere [83, 87]. Note that the catch-slip model introduces two additional parameters beyond the slip bond model, so unless there is evidence of catch bond behavior in a given system, adhesion bonds are most simply modeled as slip bonds.

9.4.3 The Molecular Clutch Hypothesis and Stiffness Sensing

The "molecular clutch" hypothesis is an established model for cell force transmission through dynamic adhesion complexes to the underlying substrate [88]. From a modeling perspective, individual clutches encompass the entire force-transmitting linkage that can engage both actin and the extracellular matrix. Bound clutches transmit force to the substrate, slowing actin retrograde flow, and permitting actin polymerization that can drive leading edge protrusion (Fig. 9.2). Modeling clutches as elastic springs connected to a deformable substrate (also modeled as an elastic spring), and employing a stochastic simulation algorithm (SSA) to model clutch binding through slip bonds (Eq. 9.4), the model of Chan and Odde [37] predicted an inverse relationship between actin retrograde flow velocity and traction forces in neuron growth cone filopodia (Fig. 9.3a). Resistance from the compliant substrate opposes the motor forces, slowing actin retrograde flow (Eq. 9.2) and increasing the unbinding rate for individual clutches (Eqs. 9.4 or 9.5).

Fig. 9.3 (continued) on a soft ECM, leading to fast actin retrograde flow ($u \approx u_{\text{max}}$) that limits leading edge advancement and spreading. Clutch bonds tend to fail spontaneously even at low load, relieving mechanical strain energy and frustrating the system's ability to achieve high force transmission. (ii) ECM of intermediate stiffness enables enough time to engage nearly all the clutches to achieve load sharing between clutches, so they can sustain larger traction forces as an ensemble before unbinding. As the last few clutches engage, the forces become large enough to cause a cascade of bond failure, a "load and fail" dynamic that can cycle indefinitely. Overall, the load sharing between clutches before failure slows actin retrograde flow ($u < u_{\text{max}}$), permits leading edge advance, and averages high force transmission. The location of this regime defines the "optimal stiffness" and depends on simulation parameters, especially numbers of motors and molecular clutches [89]. (iii) On stiff ECM, clutches build forces faster than the ensemble binding time, causing individual bound clutches to quickly detach, typically before other clutches can even engage to share the load. The resultant traction forces are low, and retrograde flow speed is near its unloaded velocity ($u \approx u_{\text{max}}$). (**b**) Simulation predictions of traction forces and actin retrograde flow speed from the motor-clutch model using a previously described parameter set [89] highlighting regimes of "frictional slippage" (i, iii) and the "optimum stiffness" (ii). (**c**) A mechanism for adhesion reinforcement that can be triggered on stiff substrates and is mediated by competing kinetic rates of clutch unbinding and talin unfolding, as described previously [78]. Clutch unbinding rates (k_{unbind}) are governed by catch-slip bond behavior (Eq. 9.4), while talin unfolding (k_{unfold}) occurs as a slip bond (Eq. 9.3). Force on an individual clutch that exceeds a threshold force (yellow star) can trigger talin unfolding, which recruits additional clutch components to the complex. This permits larger traction forces on stiff substrates and a monotonically rising traction force as a function of substrate stiffness. If clutch unbinding occurs faster than talin unfolding, no new clutch components are added, and traction forces decrease on stiff substrates, giving the biphasic dependence of traction forces on substrate stiffness, with an optimum at intermediate level

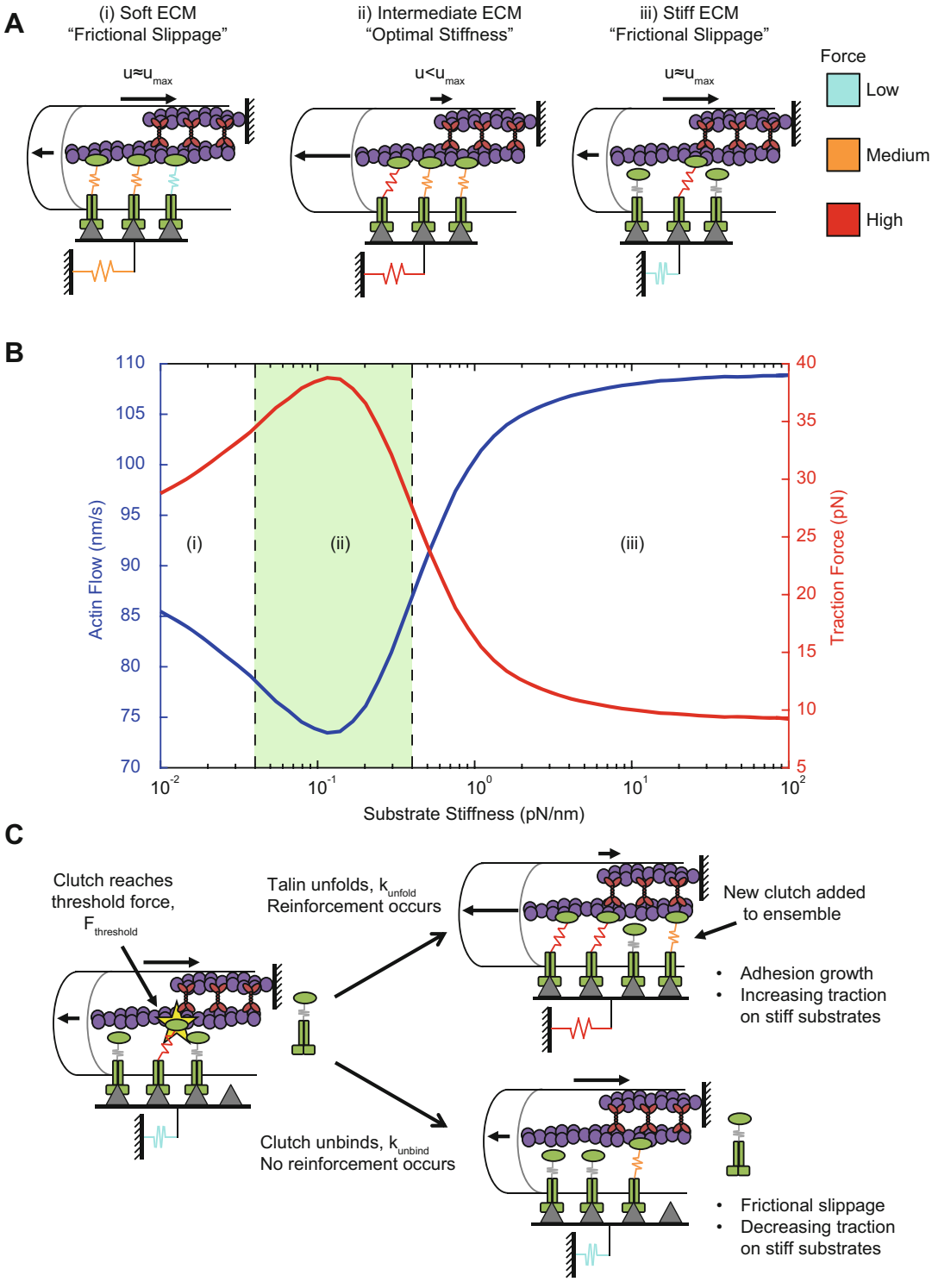

Fig. 9.3 Stiffness sensing by a molecular clutch and mechanisms of force-dependent adhesion reinforcement. (**a**) Diagrams of the molecular clutch mechanism that enables cells to sense varying ECM stiffness. (i) Actomyosin-based traction forces, established through molecular clutches (represented as springs), build slowly

The stochastic motor-clutch model predicts a biphasic response to substrate stiffness, with an "optimum" defined by maximal force generation (and minimum retrograde flow) at intermediate values (Fig. 9.3b). At the optimum stiffness, determined by model operating parameters [90], cells exhibit "load and fail" dynamics where the clutch ensemble loading time is sufficient to generate significant load before the clutches unbind and the substrate relaxes. This prediction is consistent with experimental measurements of fluctuating traction forces on compliant hydrogels [37, 91]. Inefficient force transmission and recovery of faster actin retrograde flows occurs on both softer and stiffer substrates. Soft substrates deform significantly when loaded, but clutch unbinding occurs at low forces, dissipating stored elastic strain energy and frustrating the buildup of high traction forces. Stiff substrates quickly build large forces on bound clutches, which detach before other clutches can engage to share the load, reducing overall force transmission. Both cases are termed "frictional slippage" as dissipated force allows actin retrograde flow speed to recover [89]. The optimum represents a "sweet spot" in between these extremes, where the compliant substrate affords sufficient time to engage all of the clutches yet is sufficiently stiff that they do not spontaneously disengage at low load. Solving a set of ordinary differential equations (ODE) defined by a chemical master equation, Bangasser and Odde [90] defined a critical number (N_{cr}) that defines the optimal stiffness ($\kappa_{\text{sub,opt}}$) for given model parameters.

$$N_{cr} = \frac{\kappa_{\text{sub}}}{\kappa_{\text{sub,opt}}} = \frac{\kappa_{\text{sub}} v_{\text{motor}} \ln(n)}{F_{\text{motor}} k n}. \qquad (9.5)$$

In Eq. 9.5, n refers to the number of motors and clutches, k is the clutch binding rate constant, F_{motor} is the motor stall force, and v_{motor} is the maximum motor velocity in the absence of load (Eq. 9.3). Equation 9.5 is valid assuming (i) motor and clutch numbers are approximately equal ($n_{\text{motor}} \approx n_{\text{clutch}}$), (ii) clutch binding rate exceeds the basal unbinding rate ($k_{\text{on}} \approx 10 k_{\text{off}}$), and (iii) force-dependent clutch unbinding as slip bonds (Eq. 9.4). Dimensionless analysis provides a way to quickly estimate cell responses to stiffness given their operating parameters. When $N_{cr} \approx 1$, cells are in the "load and fail" regime near the optimum, while $N_{cr} << 1$ and $N_{cr} >> 1$ are the regimes of "frictional slippage" on softer or stiffer substrates. Bangasser et al. [89] posited that this principle could explain differences in stiffness-sensitive traction force and cell migration trends among various cell lines; they would each have a different optimal stiffness as defined by the parameters in Eq. 9.5. This was experimentally confirmed in glioma cells where partial pharmacological inhibition of myosin II motors and RGD-binding integrins reduced the optimal stiffness for migration [79]. Other simple modifications to the versatile motor-clutch model framework enable theoretical studies of cell spreading dynamics on viscoelastic substrates [92] or ECM fiber assembly within tissues [93].

Other models have relied on a similar mechanical framework to the motor-clutch model. Li et al. [87] simulated a multilayer adhesion with an immobile layer of springs representing extracellular matrix ligands and intermediate layers that connect to a sliding actin filament bundle. Transient bonds within these intermediate layers reflect the observation that shearing can occur for intermediary molecules within the adhesion, as well as the adhesion receptor-ligand or adaptor-actin interfaces [73, 94]. Their model faithfully replicates the biphasic force-velocity relationship observed experimentally within adhesions [50] without requiring an empirical force-velocity relationship (Eq. 9.2). Tunable spring stiffness for each of the adhesion layers enables them to test stiffness dependence of traction forces.

9.4.4 Stick-and-Slip and Frictional Adhesion Dynamics

Other approaches to modeling the ensemble behavior of adhesions include "stick slip" dynamics. Sabass and Schwarz [95] modeled adhesions as a force balance between an actomyosin driving force (e.g., retrograde flow), intracellular viscous friction, and elastic resistance from adhesion re-

ceptors that are bound to the substrate. Using a master equation approach to model bond dynamics, their model replicates a biphasic force-velocity relationship, as well as an interesting strong dependence on intracellular friction. In the low friction case (short relaxation times), individual bond failures can trigger cascades within the adhesion leading to "stick-and-slip" behaviors that report fluctuating traction forces, reminiscent of "load and fail" dynamics [37, 91]. For longer viscous relaxation times, the adhesion generates constant forces, essentially functioning as a frictional element. Wolgemuth [38] coupled a contractile stress to stick-and-slip adhesions to reproduce regimes of persistent growth or periodic retraction, concomitant with periodic fluctuations in the concentration of a contractile chemical species within the protrusion. Sacrificing detailed binding and unbinding kinetics of individual clutches can also save computational time for models to incorporate dynamics of molecular signaling pathways. As an example, Welf et al. [96] incorporated Rac GTPase-based actin protrusion and myosin II activation from engaged clutches to capture fluctuating leading edge advance during force generation.

9.4.5 Force-Dependent Adhesion Reinforcement

Adhesion-based models discussed to this point have assumed that adhesions are a constant size, focusing instead on the efficiency of force transmission under a range of conditions [37, 87, 95] or on the spatial distribution of forces within adhesions [97]. Migrating cells have dynamic adhesions that first appear as nascent focal contacts near the leading edge, assembling and elongating under the cell as they transmit force and disassembling at the rear to permit motion of the cell body [98]. This maturation process is highly force-dependent, both on internal actomyosin forces and on mechanical resistance from stiff substrates [99–101].

Models often either set a force threshold for the individual bonds [102] or an energetic barrier to the addition of new components that is reduced by applied load [103, 104]. Cao et al. [104] modeled a force-generating actomyosin network (actuator in parallel with a spring) coupled to the nucleus at one end and an adhesion plaque at the other. Actomyosin force feedback, as well as tension within the adhesion structure, determines the flux of adhesion components that regulates adhesion length by reducing the energetic barrier for addition. Although their model does not consider adhesion protein binding and unbinding kinetics (individual adhesions are simply added or lost from the plaque), it does successfully capture tension-dependent dynamics of the adhesion life cycle and the observation of larger adhesions on stiff matrices and for cells that generate large contractile forces. Interestingly, they also predict that either stiffer nuclei or stiffer ECM will increase the number and size of adhesions by decreasing the energetic barrier for nucleation.

What molecular mechanisms enable adhesions to sense and grow in response to substrate stiffness? Many adhesion components inside the cell are directly subject to mechanical forces, so force-feedback mechanisms may function by driving tension-dependent protein conformation changes that mechanically strengthen adhesion components or activate intracellular signaling networks [18]. By adapting the properties of the adhesion as substrate resistance builds, traction forces may rise linearly with increasing substrate stiffness, as observed experimentally [78, 105], contrary to the "optimum stiffness" prediction of the motor-clutch model [89]. Although, it is important to note that there may still exist an optimum at higher stiffness than is typically examined in experiments [48]. Recent measurements of forces across integrin-containing focal adhesions clearly indicate nonuniform loads across single integrins within focal adhesions, with most individuals experiencing loads within a 1–10 pN range [85], while forces up to 40 pN have been reported [86, 106]. Nonuniform loading is expected within a retrograde flow-driven system [37], so models often assume that individual bound clutches contribute to a reinforcement signal once forces build past a defined threshold [48, 75, 78].

Elosegui-Artola et al. [78] extended the motor-clutch model [37] to include force-dependent recruitment of adhesion components. Their model features fibronectin-binding integrins that exhibit catch-slip bond behavior (Eq. 9.5) and transfer load to talin molecules within adhesions as they are stretched. The probability of talin unfolding is modeled as a slip bond (Eq. 9.4) that can unfold above a certain threshold force, determined in vitro for vinculin head binding to cryptic binding sites [107]. Unfolding signals the recruitment of additional integrins to the adhesion, effectively increasing the binding rate between integrin and fibronectin (e.g., k_{bind} between integrin and ECM, Fig. 9.2b). Consequently, traction force monotonically increases on stiff substrates. Eliminating the recruitment mechanism mediates the switch to biphasic traction and flow (Fig. 9.3c). Importantly, Elosegui-Artola et al. went on to experimentally confirm monotonically increasing traction forces as a function of substrate stiffness in the presence of talin-mediated reinforcement and the reversion to biphasic behavior in talin-depleted cells [78]. This behavior switch also coincided with nuclear recruitment of YAP transcription factor, suggesting Elosegui-Artola et al.'s results underlie a fundamental mechanosensitive signaling mechanism that regulates gene expression.

9.5 Under Pressure: Cells Migrating in Conditions of Mechanical Confinement

Although principles outlined in previous sections form the basis for the canonical model of cell migration, there are many context-dependent phenomena that may contribute to cell migration mechanics. For example, actin polymerization is not the only way cells can generate protrusive forces to migrate, and some cell types can migrate even in the absence of apparent filamentous actin structures following treatment with drugs that inhibit actin self-assembly [12]. Hydrostatic pressure within the cell can generate protrusion of membrane blebs around weak points in the actin cortex (Fig. 9.4a) leading to hyper polarized migration driven by robust cortical actin flows (Sect. 9.3) observed in confined, weakly adhesive environments (Fig. 9.4b). We next present three examples of how models could incorporate physical phenomena observed in migrating cells.

9.5.1 Blebs and Pressure-Driven Membrane Extension

Tozluoğlu et al. [108] model the plasma membrane as an elastic layer connected to a viscoelastic actin cortex. Changes in intracellular hydro-

Fig. 9.4 (continued) feedback mechanism enhances fluctuations in cortical tension within blebs, leading to the establishment of fast cortical actin flows (u_{cortex}) and actin density gradient that are reinforced by actin turnover within the bleb. Anisotropic cortex tension, due to the polarized distribution of actin filaments, is required to initiate this symmetry breaking mechanism. (**c**) Intracellular pressure can also drive cellular protrusion in dense ECM conditions that mechanically confines the nucleus, known as the "nuclear piston" hypothesis [109]. When the nucleus occludes a pore, actin-myosin contraction can increase P_{cell} in the isolated front of the cell, fueling pressure-driven extension of the cell front into gaps in the ECM. P_{cell} remains low in the cell rear. If nucleus-cytoskeleton linkages (yellow) are disrupted, the piston mechanism is not activated, since weak nuclear anchoring can allow pressures to equilibrate between the two compartments. This provides an alternative, pressure-based mode of protrusion that can supplement actin polymerization under these confinement conditions. (**d**) Schematic of cell migration in confined channels driven by intracellular osmotic and hydrostatic pressures, as described by an osmotic engine model [12]. A polarized distribution of ion pumps establishes ion fluxes on the leading (J_{in}) and trailing (J_{out}) ends of the cell. This creates an osmotic pressure change ($\Delta\pi_{\text{ion}}$) and hydrostatic pressure change (ΔP_{cell}) between the leading and trailing edges of the cell that pushes the leading membrane forward. Friction between flowing cytoplasm, cell cortex, and channel wall enables force transmission and forward motion of the cell within the channel

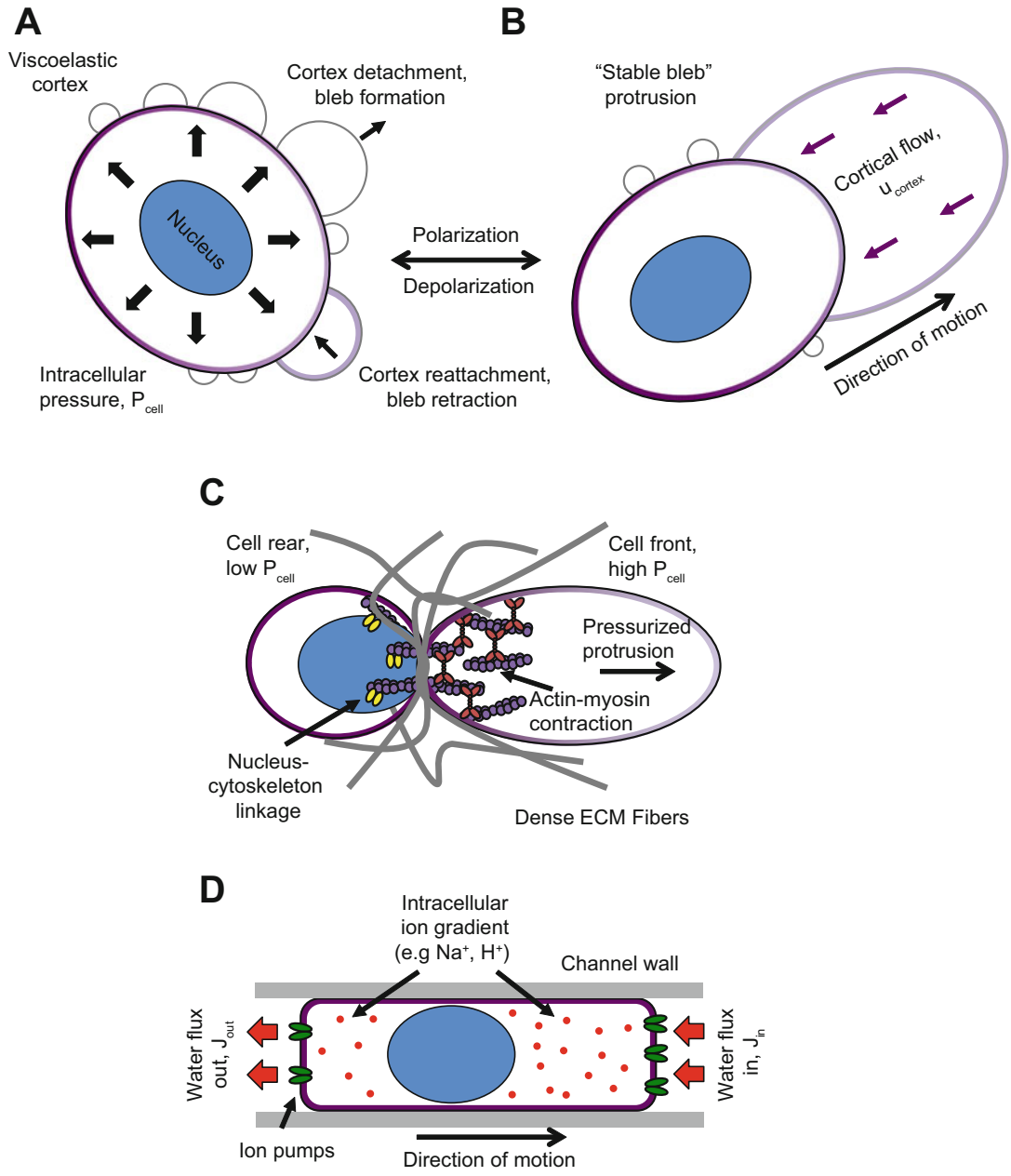

Fig. 9.4 Pressure-driven modes of cell protrusion and migration in conditions of high contractile forces or mechanical confinement. (**a**) Schematic of the mechanical process of bleb formation, featuring a viscoelastic actin cortex (shaded purple) coupled to an elastic membrane (gray), based on a hybrid agent-based/finite element model (FEM) of cell migration [108]. Intracellular pressure (P_{cell}) at weak points in the cortex-membrane cohesion can cause the membrane to delaminate, driving protrusion by membrane blebs. Blebs are limited by membrane elasticity and retract when the actin-myosin cortex reforms. This mechanism is distinct from actin-based protrusions, which contain an intact cortex layer during the process of elongation and/or adherence to the ECM. (**b**) Spontaneous "stable bleb" protrusion can drive cells toward highly polarized migration, as previously described using FEM [62]. An actin-myosin force

static pressure and cortical tension allow their model to capture the rapid expansion and slow retraction dynamics of blebs under conditions such as high contraction forces or weak cortical engagement (Fig. 9.4a). This approach faithfully replicates shapes of migrating cancer cells imaged using intravital imaging and enables them to infer regimes where protrusive steps in migration are dominated by either actin-based protrusions (Fig. 9.1) or pressure-based (blebbing) motility (Fig. 9.4b). The latter primarily occurs when the membrane layer (elastic spring) delaminates from the viscoelastic cortex (modeled as a Kelvin-Voigt spring and dashpot), leading to rapid expansion into gaps between ECM fibers (which they explicitly include in their model, but are not pictured in the schematic in Fig. 9.4a, b). One critique of their model, however, is that the two-layer cortex fails to include robust actin flows (Fig. 9.4b) that are often observed in highly polarized, fast migrating cells [51, 61, 62].

Intracellular pressure also plays a role in protrusion dynamics even within strongly adhesive environments, such as dense extracellular matrix. In these environments, the ECM is typically quite dense, forcing cells to squeeze through constrained pores; the largest dimension in these spaces can be ~1 μm or less [21]. When the nucleus occludes a pore smaller than its dimension (typically ~5 μm), protrusions can become pressurized by actomyosin contraction, driving fast leading edge extension into the extracellular space [109]. This "nuclear piston" mechanism depends on nucleus-cytoskeleton linkages, substrate adhesion, and actomyosin force generation [110] and provides cells moving through confined ECM pores with another means of driving fast leading edge propulsion. Although the nuclear piston has not yet been incorporated into mathematical models of cell migration, pressure-driven protrusions could be modeled alongside actin dynamics by reducing the stall force on polymerizing filaments, contributing an additional protrusive force to leading edge extension [111].

9.5.2 Confined Migration Driven by Osmotic Pressure

Cells are also quite sensitive to influences from osmotic pressures generated by ion species in their environment. Stroka et al. [12] demonstrated that tumor cells in narrow (30 μm^2) microfabricated channels were insensitive to myosin II and actin polymerization inhibitors that block migration on 2D substrates and in wider channels, but disruption of aquaporins or ion channels slowed migration. In their model (the Osmotic Engine Model), a polarized distribution of ion pumps drives a net inward water and ion flux (J_{in}) at the cell front and a net outward flux (J_{out}) at the rear through semipermeable cell membranes (Fig. 9.4d). Water and ion fluxes drive osmotic and hydrostatic pressure gradients within the cell, pushing the membrane forward, while viscous friction between the cortex and cytoplasm and between the cortex and channel walls resists forward motion within the channel. The Osmotic Engine Model quantitatively predicts cell velocity responses to osmotic pressure changes on either the leading or trailing edge of the cell, demonstrating a possible heightened role of osmotic pressure-driven tumor cell migration in dense tissues. Two major caveats to the Osmotic Engine Model are that (1) model predictions were only tested on cells experiencing a high degree of confinement in vitro in devices fabricated from (stiff) elastomer materials, and (2) this type of pressure-driven migration mode may only apply to certain tumor cell types with high expression levels of certain ion pumps. The model also does not incorporate principles of actomyosin-based forces that cells often use. Combined with other models that incorporate actin, myosin, and adhesions, the Osmotic Engine Model may provide an asymmetry in forces on the plasma membrane, leading to reduced compression on actin filament barbed ends at the leading edge relative to the trailing edge and concomitant net asymmetry in actin assembly.

9.5.3 Mechanical Roles of the Cell Nucleus

The nucleus is the largest organelle in the cell; it is relatively stiff (1–10 kPa) and can experience viscoplastic deformation, all of which may present a steric challenge for cells in dense tissue environments. As such, the nucleus impedes cell migration through constricted pores, and passage times depend on nuclear mechanical properties [112, 113]. Cells can adopt a range of pushing and pulling mechanisms to move the nucleus, typically involving actin-myosin pushing forces [17], large traction forces within leading protrusions [48], internal microtubule motor-based forces [114], or by using actin polymerization to drive nuclear shape changes [115]. Cao et al. [116] coupled a contractile cell cytoskeleton to a deformable nucleus in order to simulate nuclear deformation during transmigration through a stiff endothelial barrier, as may occur during metastasis. They model the nucleus as a thin elastic shell filled with poroelastic material, which reproduces mechanical stresses and plastic deformations observed in experiments, while ECM stiffness and pore size emerged as major determinants of transmigration efficiency. Similar models apply finite element modeling (FEM) to create a cell consisting of two viscoelastic layers (nucleus and cytoplasm) and generates cyclic contractile forces to replicate the stresses involved in deforming the nucleus and cytoskeleton as it enters a rigid-walled microchannel [117]. Coupled to other models of cell migration, nuclear forces could also be modeled as potential energy barriers that contribute resistive forces to cell motion, in order to replicate the mechanical challenge of overcoming tissue barriers.

9.6 Whole-Cell Migration Models: Force-Balances and Motion

While many models, such as the motor-clutch model, describe only one part of a cell, such as a lamellipodial or filopodial protrusion (Sect. 9.2), or the force dynamics of a single focal adhesion complex (Sect. 9.4), more generally we seek to develop models that capture whole-cell dynamics during migration. We define whole-cell models as those that integrate physical principles of force balances and mass conservation to facilitate motion, and we review a few key examples of such below.

9.6.1 Adhesiveness Defines Biphasic Cell Velocity

Seminal modeling work by DiMilla et al. [6] coupled intracellular transport and recycling of adhesion receptors that enforce polarity to a mechanical model of a cell moving in 1D on an adhesive substrate (Fig. 9.5a). Their simulated cell consisted of several mechanical elements, each containing force-generating elements coupled to a viscoelastic cytoskeleton, which undergoes force generation cycles. Each mechanical element was also coupled to a set of adhesion receptors modeled as elastic springs with an intrinsic stiffness. Receptor binding is at equilibrium (constant traction force) because the binding and unbinding times are small compared to the cycle time for force generation. Asymmetric receptor number at the cell front and rear gives rise to motion (an implied polarization of the cell) and enables calculation of cell velocity for varying quantities such as traction force or adhesive ligand concentration. A transport model for adhesion receptor endocytosis and trafficking maintains cell polarization.

Although their model assumes an infinitely stiff substrate, implied polarity, and uses averaging behavior of adhesion dynamics (ignoring the contributions of individual bonds), they are still able to make several important predictions of cell behaviors. Notably, their model reproduces an experimentally observed biphasic relationship between cell speed and adhesive ligand concentration ([L], termed "adhesiveness") for a given contractile force output by the cell [118, 119]. Cells in poorly adhesive environments (low [L]) migrate slowly, since the few available bonds insufficiently support traction forces. Cell migration is also slow in strongly adhesive envi-

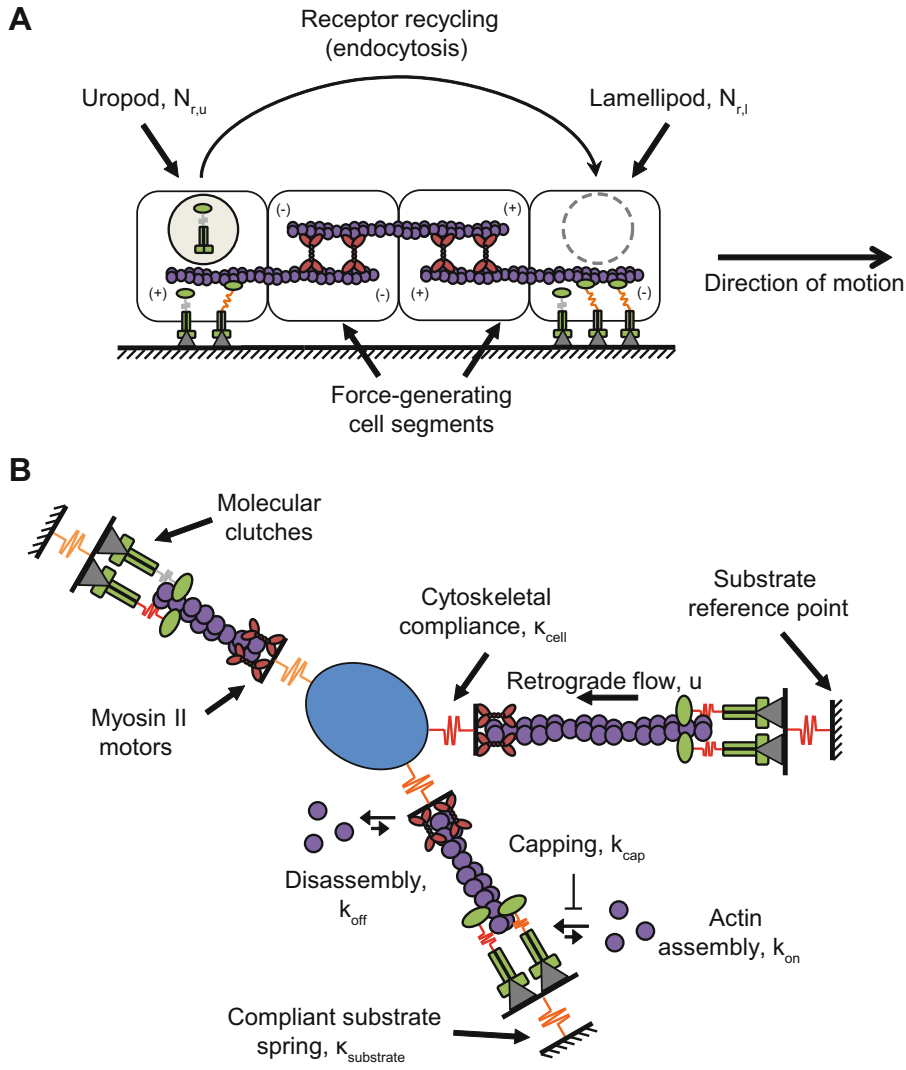

Fig. 9.5 Whole-cell models of cell migration that integrate mechanical steps to reproduce cellular behaviors. (**a**) An integrated 1D whole-cell migration model [6], which couples a mechanical model of cell adhesion and contractile force generation to a transport-based model of adhesion receptor endocytosis. A migrating cell consists of modules representing a leading edge (lamellipod) and trailing edge (uropod) and bridging contractile elements between the two. Contractile elements each contain a viscoelastic cytoskeletal element and active force generator (spring, dashpot, and contractile element in parallel). The lamellipod and uropod contain a viscoelastic cytoskeletal element (spring and dashpot in parallel) and the number of adhesion receptors ($N_{r,l}$ and $N_{r,u}$, respectively) which can dynamically bind and unbind ligands on the cell substrate. Unbound receptors near the cell rear are trafficked by endocytosis to maintain a polarized distribution that favors adhesion at the cell leading edge. Bound receptors transmit contractile forces to enable polarized movement of the cell. (**b**) Schematic of a stochastic cell migration simulator [79] based on the motor-clutch model described in Figs. 9.2 and 9.3. Simulated cells consist of a central cell body, coupled to protrusions by springs (κ_{cell}) representing nucleo-cytoskeletal compliance. Modules contain motors and clutches and are, in turn, coupled to compliant substrate springs ($\kappa_{substrate}$) at the ends of modules. Motors generate retrograde flow (u), which establishes traction forces through bound molecular clutches that extend the compliant substrate. Force balances between traction forces and the cell body guide random motion of the cell. Actin assembly allows protrusion extension, while retrograde flow drives module shortening and returns actin to the central pool. A mass balance between actin filaments and unassembled actin (Eq. 9.6) limits the total extension of the cell modules. Modules are stochastically capped (k_{cap}) and excluded from actin assembly to facilitate turnover and cell motion. Actin-dependent nucleation (k_{nuc}), in turn, generates new modules (not pictured)

ronments (high [L]), because the high concentration of available ligand ensures that unbound receptors quickly rebind, effectively stalling cell motion. Fastest migration occurs at intermediate ligand density, yielding a trend that is similar to the biphasic stiffness sensitivity observed for traction forces in the motor-clutch model (Fig. 9.3b). DiMilla et al.'s model provided an important blueprint to integrate the chemical and mechanical steps of protrusion, contraction, and adhesion and to probe the role of ECM properties in guiding migration.

9.6.2 Modeling 2D Random Migration

Migrating cells can adopt a wide range of motility behaviors on unconstrained 2D environments in the absence of directional mechanical or chemical cues, from the highly persistent motion of keratocytes to random walk behavior characteristic of mesenchymal cells. In order to replicate 2D random motion, mathematical models have tended to rely on a stochastic simulation framework with random events corresponding to changes in polarization direction. Tranquillo et al. [120] compared cases of leukocytes in chemoattractant gradient to motion in the absence of directional cues. They modeled a leukocyte as a polarized two-part lamellipodium containing chemoattractant receptors, which can fluctuate between sides in response to cues. Receptors with bound ligand steer cell motion in a particular direction, based on their relative spatial position within the lamellipodium, and proportional to their relative distribution between the two sides. Capitalizing on these principles, and the integrated chemical and mechanical model of DiMilla et al. [6], subsequent modeling efforts by Dickinson and Tranquillo [5] used a stochastic differential equations (SDE) model to determine a similar relationship for adhesion receptor binding coupled to cell directionality. Intracellular receptor transports to various cell regions, and adhesion receptor binding kinetics determines the spatial distribution of forces that guide motion. Akin to DiMilla et al. [6], their model considers an infinitely stiff substrate and fixed cell polarity and faithfully reproduces the adhesiveness relationship. Using this model, Dickinson and Tranquillo [5] demonstrated the capacity of stochastic methods to reproduce 2D cell trajectories similar to experiments.

9.6.3 3D Migration Models

Developing detailed, accurate models of 3D cell migration relies on a similar set of principles to these discussed previously, although the role of realistic tissue environments may provide additional cues that are not present on flat 2D substrates. Tissue ECM may have strongly anisotropic mechanical properties, presenting cells with constricted pores or aligned fiber structures, as well as temporally varying chemical cues [16]. Cells employ diverse alternative "modes" of navigating these environments, such as fast "leader bleb" migration in poorly adhesive environments [51] or osmotic pressure-driven migration in stiff, confined channels [12], although well-established phenomena such as the molecular clutch likely still apply in many cases [121]. We have presented some ideas in earlier sections that could account for conditions such as confinement of the nucleus (Sect. 9.5.3), but many of these conditions remain to be rigorously tested within migration models.

Zaman et al. [122] constructed a 3D migration model that incorporates elements of protrusion, force generation, and viscoelastic ECM properties into the framework of a single cell. Protrusions are generated stochastically in random directions (enabling spontaneous repolarization of the cell on a relevant timescale) and each protrusion capable of generating traction forces that are summed to a total force on the central cell body. Drag forces from a viscoelastic ECM resist protrusive forces, providing a means to empirically account for confinement conditions that slow migration. Their approach has several limitations, namely, that the model

does not contain a force-velocity relationship for traction force generation, relies on a longtime step that requires "coarse-graining" of protrusion dynamics and adhesion bond engagement, and requires an implied polarity by asymmetric distribution of adhesion receptors. Furthermore, assuming a 3D isotropic environment ignores anisotropic tissue features, such as aligned collagen fibers, which may have mechanical properties that change based on loading conditions [123] and can serve as "tracks" that bias cell migration in a particular direction [124]. Their model does, however, successfully predict migration velocity trends of carcinoma cells in manufactured 3D ECM environments where adhesion receptor number and ECM stiffness were independently varied in experiments [125].

9.7 Relating Physical Models to Tumor Progression and Treatment

To this point, our discussion has primarily focused on models that capture the cellular dynamics of migration. Modeling has been successful in elucidating physical phenomena within cells and creating models that faithfully predict results of in vitro experiments. We have also discussed opportunities for models to incorporate ECM properties such as stiffness, composition, and architecture, which can influence cell behavior. Many of these properties may vary widely between healthy and tumorigenic tissue, or between tissue types, as metastatic cells colonize new organs [126], so it is important to incorporate these effects in order to guide better strategies for clinical management of invasive tumors. In this next section, we introduce recent modeling efforts from our laboratory toward using the motor-clutch model (Sect. 9.4.4) as a general framework for predicting biophysical properties of malignant cells, as well as disease progression in cancer models and human disease. We next provide context for implementing models to predict disease-relevant cell migration behaviors.

9.7.1 Cell Migration Simulator: Stiffness-Sensitive Migration via a Motor-Clutch Model

Migrating cells are responsive to changes in bulk tissue stiffness, to which many cells are quite sensitive. For many cell types, there exists a biphasic response to stiffness, where migration speed or random motility coefficient is fastest on intermediate stiffness and slow on softer or stiffer [79, 127, 128]. Tissue environments may also present cells with mechanical stiffness gradients, and durotaxis refers to the propensity of certain cells to bias migration behavior in order to follow these gradients [129]. Building on the stiffness-sensitive traction force framework of the motor-clutch model [37], a cell migration simulator (CMS) was recently designed to capture cell migration trends in environments with varying chemistry and mechanics [79, 118].

The CMS (Fig. 9.5b) is built upon fundamental principles described in previous sections, integrating the motor-clutch model (Sect. 9.4.4) with actin protrusion kinetics and turnover. Individual protrusions, each functioning according to the motor-clutch model, adhere to a compliant substrate spring at one end. The other end is fixed to the central cell body by an elastic spring that represents the compliance of the cell and which adheres to the substrate by a set of cell body clutches (which follow the same rules as module clutches, but are not subject to direct motor forces). Modules undergo elongation by actin polymerization and shortening by retrograde flow, destroyed when they shorten below a threshold length (facilitated by stochastic capping, which terminates extension by actin polymerization) and stochastically generated at a rate determined by the free actin concentration. Total actin (A_{total}) is constrained by mass conservation between the free concentration (A_G) and filament (A_F) states, as given in Eq. 9.6.

$$A_{\text{total}} = A_G + \sum_{j=1}^{n_{\text{mod}}} A_{F,j} \tag{9.6}$$

Equation 9.6 represents a cell with j modules, each containing a certain length of filamentous actin and a pool of monomers (representing the free concentration), constrained by A_{total}. An SSA [130] guides simulation progression by randomly selecting events such as clutch binding or unbinding, module birth, or capping, while a force balance on modules and the cell body updates cell centroid and reference positions at each simulation step. The stochastic nature of the simulation replicates individual random trajectories (as well as quantities such has traction force, actin retrograde flow, and aspect ratio) using a unique random number "seed" for each simulated cell, facilitating comparison to experimental data sets [79, 118]. In subsequent sections, we provide examples from recent literature for how models such as the motor-clutch model or CMS may be used to predict biophysical mechanisms of cancer progression or treatment.

9.7.2 Parameterizing Tumor Cells with Experimental Data

Tissue stiffening around breast tumors presents migrating cells with a dense ECM that they must navigate in order to migrate [131]. Mekhdjian et al. [48] found that treatments with tumor growth factor beta (TGFβ) meant to induce an epithelial-to-mesenchymal transition (EMT) enabled cells to spread and establish large traction forces on stiff substrates, which was not observed in their untreated counterparts. Increased traction forces in either induced EMT or malignant mouse tumor cells were consistent with increased invasion into stiffened 3D collagen matrices. Complementary experiments measured pN-scale forces using molecular tension sensors [85, 132], sensitive molecular probes designed for single integrin force measurements. Cells also had reduced traction force output and spreading on stiff substrates, consistent with a regime of frictional slippage (Fig. 9.5). The motor-clutch model provided quantitative estimates of traction forces and spread areas (estimated using a mass balance on actin, as in Eq. 9.6) for both control and TGFβ-treated epithelial cells, consistent with an increased optimal stiffness for malignant cells [48]. Increased traction forces were most readily explained by increases in both motor and clutch number (which increases the optimal stiffness, by Eq. 9.5) and found to be the strongest biophysical predictor of 3D collagen invasiveness and passage time through subnuclear scale constrictions. Thus, a hypothetical treatment aimed at curbing migration on stiff diseased tissue could aim to reduce motor and clutch number.

9.7.3 Correlating Cell Adhesion with Tumor Progression

Integrins and adhesion proteins are often dysregulated in tumors [48, 71, 133] and represent possible targets to curb motility. One such example is the glycoprotein receptor CD44, which functions as a signaling molecule and putative clutch molecule for hyaluronic acid (HA) [68], which is a major component of brain ECM [134]. In the case of glioblastoma (GBM) brain tumors, CD44 could be a critical element of the GBM cell adhesion machinery that enables invasion into HA-rich brain regions. CD44 expression has a complex history as a prognostic factor for GBM, with some studies reporting negative correlation with disease survival [135], some positive correlation [136], and some no correlation [137]. Using engineered GBM mouse models with varying CD44 expression backgrounds, Klank et al. [118] reported a biphasic cell migration speed that is inversely correlated with mouse survival: mice with low or high CD44 expression have the longest survival, while the intermediate-expression groups fare worst. By varying the clutch number against a fixed motor number in the CMS, they replicated the biphasic "adhesiveness" relationship (Sect. 9.6.1) first theoretically described by DiMilla et al. [6]. Importantly, their results hold for a compliant environment and without an imposed polarization of the cell. A biphasic fit also correlates CD44 expression with disease survival in patient biopsies from multiple GBM subtypes and reconciles the previous discrepancies in using CD44 expression to predict disease outcome [118].

9.7.4 Interpreting or Predicting Effects of Motility-Targeting Drugs

Treatments aimed at curbing cell motility are a promising concept for cancer treatment [138, 139], suggesting their effective implementation benefits from increased knowledge of cell migration mechanisms. However, in practice, their theoretical promise can exceed their actual performance in clinical trials. Cilengitide, a cyclic peptide that contains the arginine-glycine-aspartic acid (RGD)-binding site recognized by $\alpha_v\beta_3$ integrins, recently completed a Phase III trial in glioblastoma while providing no benefit compared to standard of care [71, 140, 141]. As discussed previously (Sect. 9.7.3), a treatment designed to inhibit adhesion molecules may yield mixed results, depending on the expression of that particular adhesion molecule in tumor cells.

Biphasic cell migration response to CD44 expression [118] suggests that a hypothetical anti-CD44 therapy would have the greatest benefit for the intermediate-expressing cohort; low-expressing patients already have improved survival corresponding to slow migration, while intermediate-expressing patients could be shifted to the low-expressing regime. In the high-expressing cohort, the same anti-CD44 therapy would run the risk of increasing cell migration speed due to only partial inhibition, fueling tumor progression and shortening patient survival times. If one averages the three hypothetical outcomes—improved, no effect, and worsened—then there may not be an overall benefit. By contrast, model-driven stratification of patients to focus on the group most likely to benefit (the intermediate CD44-expressing group, in this case) could lead to better clinical success. Observation of a biphasic adhesiveness relationship in vivo and corresponding to CD44 expression in human patients suggests that simple biophysical theory can have meaningful implications for treatment response. Model-predicted adhesion effects should thus be considered in designing future clinical trials aimed at targeting cancer cell motility.

Bangasser et al. [79] have similar implications for cells migrating on stiffened ECMs that are frequently associated with aggressive tumors [142–146]. Using human glioma cells, they showed that fastest migration occurs on PAG hydrogels of 100 kPa modulus. Upon simultaneous inhibition of myosin II motors and integrin-mediated clutches, migration speed increased on softer PAGs (1–10 kPa) while decreasing at 100 kPa. Reducing the number of motors and clutches in the CMS (while holding all other parameters constant) produced a similar shift in optimal migration to lower stiffness. Individual drugs shift cells to a "stalled" or "free-flowing" regime when a myosin II or integrin inhibitor is added, respectively [79]. "Stalled" refers to the condition where cells strongly adhere to their environment and is characterized by maximal traction forces (i.e., $F = F_{\text{stall}}$) and slow retrograde flow. The "free-flowing" regime occurs when motor forces are much stronger than adhesions can resist, leading to rounded cells, fast flows, and reduced traction forces. Both cases can abolish the stiffness sensitivity of cell tractions and retrograde flow velocity predicted by the motor-clutch model [89].

In therapeutic terms, this indicates that a hypothetical combination therapy of two drugs, one targeting motors and one targeting clutches, could slow tumor cell migration on stiffened ECM, thus resulting in slower disease progression without changing the migration "mode" employed by invading cells. Single drug therapies may fail when cells have a means of adapting their migration machinery to the new environment—for example, reduced cell adhesion may cause a "mesenchymal-to-amoeboid transition" (MAT) that recovers motility in contractile tumor cells [51]. A general modeling framework can allow us to better predict cell responses to therapy and could be integrated into clinical studies.

9.7.5 Toward Emergent Multicellular Behaviors

The primary focus of this chapter has been on efforts to model single cell migration behaviors and properly representing the underlying molecular mechanisms in physical models. We have outlined some ways differences between cells could be parameterized in models, but have not discussed collective multicellular behaviors. Although single cell dissemination occurs in tumor progression and may contribute to tumor spreading, multicellular collective modes have also been observed in tumor invasion, as well as healthy functions such as wound healing and tissue formation [1]. Cells within tissues are often bound to other cells through intercellular junctions; these contain adhesion proteins such as cadherins [67], which bear mechanical forces through cytoskeletal connections [147]. Binding dynamics for cadherins and other cell-cell adhesion proteins may exhibit properties similar to cell-ECM bonds, such as catch-slip behaviors [82], and thus their dynamics would follow similar behaviors as previously discussed (Sect. 9.4.2). Significant experimental efforts have recently been directed at elucidating physical phenomena such as "jamming" that occurs within densely packed cell layers [148, 149], but few models have made efforts to model collective behaviors while still rigorously capturing intracellular force generation fundamentals discussed in this chapter. One simple interpretation is that collectives may represent a way for a group of cells to effectively act as a single large cell and thereby increase their relative numbers of motors and clutches [89], enabling faster migration or other stiffness-sensitive behaviors in stiffened ECM.

Sunyer et al. [150] adapted the clutch model framework to account for collective durotaxis of cell sheets. Their model considers a cell sheet as a long 1D truss element that generates contractile forces, while adhesion complexes (modeled as slip and catch-slip bonds) engage actin filaments and a continuous substrate of varying stiffness at either end of the sheet. Protrusion at either end of the cell is governed by both actin polymerization and deformation of the compliant substrate. When the substrate contains a stiffness gradient, the sheet moves toward the stiffer, less deformable regions, reconciling earlier descriptions of durotaxis [129]. Disrupting cell-cell junctions by protein knockdown impaired durotaxis and could be replicated in the model by replacing rigid cell-cell junctions with compliant springs, reducing end-to-end force transmission. The Sunyer et al. model is an important step toward modeling collective cell migration behaviors without sacrificing molecular-scale detail or physical principles.

9.8 Conclusions: Mathematical Models as Oncology Tools

Biophysical modeling is a powerful tool, both for its capacity to interface with experimental data and to predict cellular behaviors that elude traditional intuition. Modeling shares a rich history with cell biology, as numerous landmark papers over the last few decades have yielded critical physical insights into the fundamental mechanics of migrating cells. Now, cutting-edge microscopy methods, gene editing and protein engineering techniques, molecular force sensors, and biomaterials with tunable mechanics and chemistry enable modelers' mechanistic predictions to be tested in unprecedented molecular detail. Moving forward, we argue that effective models should not merely describe a set of experiments; they should also guide experimental design that predicts novel and potentially non-intuitive cellular behaviors. Herein lies the potential for oncology research: well-designed models should make testable predictions related to disease progression or suggest "weak points" in the cell migration machinery that can be therapeutically exploited to yield favorable patient outcomes.

Acknowledgments The authors thank Ghaidan Shamsan and Brian Castle for their input in creating the figures and organizing the chapter. Louis S. Prahl acknowledges funding from an NSF Graduate Research Fellowship grant 00039202. David J. Odde acknowledges funding from NIH grants R01 CA172986 and U54 CA210190.

Bibliography

1. Friedl P, Gilmour D (2009) Collective cell migration in morphogenesis, regeneration and cancer. Nat Rev Mol Cell Biol 10(7):445–457
2. Ridley AJ, Schwartz MA, Burridge K, Firtel RA, Ginsberg MH, Borisy G, Parsons JT, Horwitz AR (2003) Cell migration: integrating signals from front to back. Science 302(5651):1704–1709
3. Weigelt B, Peterse JL, van 't Veer LJ (2005) Breast cancer metastasis: markers and models. Nat Rev Cancer 5(8):591–602
4. Abercrombie M (1980) The Croonian lecture, 1978: the crawling movement of metazoan cells. Proc R Soc Lond B Biol Sci 207(1167):129–147
5. Dickinson RB, Tranquillo RT (1993) A stochastic model for adhesion-mediated cell random motility and haptotaxis. J Math Biol 31(6):563–600
6. DiMilla PA, Barbee K, Lauffenburger DA (1991) Mathematical model for the effects of adhesion and mechanics on cell migration speed. Biophys J 60(1):15–37
7. Friedl P, Wolf K (2010) Plasticity of cell migration: a multiscale tuning model. J Cell Biol 188(1): 11–19
8. Lämmermann T, Bader BL, Monkley SJ, Worbs T, Wedlich-Söldner R, Hirsch K, Keller M, Förster R, Critchley DR, Fässler R, Sixt M (2008) Rapid leukocyte migration by integrin-independent flowing and squeezing. Nature 453(7191):51–55
9. Renkawitz J, Schumann K, Weber M, Lämmermann T, Pflicke H, Piel M, Polleux J, Spatz JP, Sixt M (2009) Adaptive force transmission in amoeboid cell migration. Nat Cell Biol 11(12):1438–1443
10. Bergert M, Erzberger A, Desai RA, Aspalter IM, Oates AC, Charras G, Salbreux G, Paluch EK (2015) Force transmission during adhesion-independent migration. Nat Cell Biol 17(4): 524–529
11. Le Berre M, Liu YJ, Hu J, Maiuri P, Bénichou O, Voituriez R, Chen Y, Piel M (2013) Geometric friction directs cell migration. Phys Rev Lett 111(19):198101
12. Stroka KM, Jiang H, Chen SH, Tong Z, Wirtz D, Sun SX, Konstantopoulos K (2014b) Water permeation drives tumor cell migration in confined microenvironments. Cell 157(3):611–623
13. Roca-Cusachs P, Conte V, Trepat X (2017) Quantifying forces in cell biology. Nat Cell Biol 19(7):742–751
14. Pelham RJ, Wang Yl (1997) Cell locomotion and focal adhesions are regulated by substrate flexibility. Proc Natl Acad Sci U S A 94(25):13661–13665
15. Provenzano PP, Eliceiri KW, Campbell JM, Inman DR, White JG, Keely PJ (2006) Collagen reorganization at the tumor-stromal interface facilitates local invasion. BMC Med 4(1):38
16. Charras G, Sahai E (2014) Physical influences of the extracellular environment on cell migration. Nat Rev Mol Cell Biol 15(12):813–824
17. Beadle C, Assanah MC, Monzo P, Vallee R, Rosenfeld SS, Canoll P (2008) The role of myosin II in glioma invasion of the brain. Mol Biol Cell 19(8):3357–3368
18. Hoffman BD, Grashoff C, Schwartz MA (2011) Dynamic molecular processes mediate cellular mechanotransduction. Nature 475(7356):316–323
19. Condeelis J, Segall JE (2003) Intravital imaging of cell movement in tumours, Nat Rev Cancer 3(12):921–930
20. Wolf K, Alexander S, Schacht V, Coussens LM, von Andrian UH, van Rheenen J, Deryugina E, Friedl P (2009) Collagen-based cell migration models in vitro and in vivo. Semin Cell Dev Biol 20(8):931–941
21. Paul CD, Mistriotis P, Konstantopoulos K (2017) Cancer cell motility: lessons from migration in confined spaces. Nat Rev Cancer 17(2):131–140
22. Stroka KM, Gu Z, Sun SX, Konstantopoulos K (2014a) Bioengineering paradigms for cell migration in confined microenvironments. Curr Opin Cell Biol 30:41–50
23. Danuser G, Allard J, Mogilner A (2013) Mathematical modeling of eukaryotic cell migration: insights beyond experiments. Annu Rev Cell Dev Biol 29:501–528
24. Pollard TD, Borisy GG (2003) Cellular motility driven by assembly and disassembly of actin filaments. Cell 112(4):453–465
25. Svitkina TM, Borisy GG (1999) Arp2/3 complex and actin depolymerizing factor/cofilin in dendritic organization and treadmilling of actin filament array in lamellipodia. J Cell Biol 145(5):1009–1026
26. Wu C, Asokan SB, Berginski ME, Haynes EM, Sharpless NE, Griffith JD, Gomez SM, Bear JE (2012) Arp2/3 is critical for lamellipodia and response to extracellular matrix cues but is dispensable for chemotaxis. Cell 148(5):973–987
27. Abraham VC, Krishnamurthi V, Taylor DL, Lanni F (1999) The actin-based nanomachine at the leading edge of migrating cells. Biophys J 77(3): 1721–1732
28. Gittes F, Mickey B, Nettleton J, Howard J (1993) Flexural rigidity of microtubules and actin filaments measured from thermal fluctuations in shape. J Cell Biol 120(4):923–934
29. Hill TL (1981) Microfilament or microtubule assembly or disassembly against a force. Proc Natl Acad Sci U S A 78(9):5613–5617
30. Mogilner A, Oster G (1996) Cell motility driven by actin polymerization. Biophys J 71(6):3030–3045
31. Peskin CS, Odell GM, Oster GF (1993) Cellular motions and thermal fluctuations: the Brownian ratchet. Biophys J 65(1):316–324

32. Dickinson RB, Caro L, Purich DL (2004) Force generation by cytoskeletal filament end-tracking proteins. Biophys J 87(4):2838–2854
33. Mogilner A, Edelstein-Keshet L (2002) Regulation of actin dynamics in rapidly moving cells: a quantitative analysis. Biophys J 83(3):1237–1258
34. Mattila PK, Lappalainen P (2008) Filopodia: molecular architecture and cellular functions, Nat Rev Mol Cell Biol 9(6):446–454
35. Schoumacher M, Goldman RD, Louvard D, Vignjevic DM (2010) Actin, microtubules, and vimentin intermediate filaments cooperate for elongation of invadopodia. J Cell Biol 189(3):541–556
36. Vignjevic D, Montagnac G (2008) Reorganisation of the dendritic actin network during cancer cell migration and invasion. Semin Cancer Biol 18(1):12–22
37. Chan CE, Odde DJ (2008) Traction dynamics of filopodia on compliant substrates. Science 322(5908):1687–1691
38. Wolgemuth CW (2005) Lamellipodial contractions during crawling and spreading. Biophys J 89(3):1643–1649
39. Murrell M, Oakes PW, Lenz M, Gardel ML (2015) Forcing cells into shape: the mechanics of actomyosin contractility. Nat Rev Mol Cell Biol 16(8):486–498
40. Prost J, Jülicher F, Joanny J (2015) Active gel physics. Nat Phys 11(2):111–117
41. Salbreux G, Charras G, Paluch E (2012) Actin cortex mechanics and cellular morphogenesis. Trends Cell Biol 22(10):536–545
42. Janmey PA, Hvidt S, Käs J, Lerche D, Maggs A, Sackmann E, Schliwa M, Stossel TP (1994) The mechanical properties of actin gels. Elastic modulus and filament motions. J Biol Chem 269(51):32503–32513
43. Jülicher F, Kruse K, Prost J, Joanny J (2007) Active behavior of the cytoskeleton. Phys Rep 449(1-3):3–28
44. Aratyn-Schaus Y, Gardel ML (2010) Transient frictional slip between integrin and the ECM in focal adhesions under myosin II tension. Curr Biol 20(13):1145–1153
45. Lin CH, Espreafico EM, Mooseker MS, Forscher P (1996) Myosin drives retrograde F-actin flow in neuronal growth cones. Neuron 16(4):769–782
46. Mogilner A, Oster G (2003) Force generation by actin polymerization II: the elastic ratchet and tethered filaments. Biophys J 84(3):1591–1605
47. Molloy JE, Burns JE, Kendrick-Jones J, Tregear RT, White DC (1995) Movement and force produced by a single myosin head. Nature 378(6553):209–212
48. Mekhdjian AH, Kai F, Rubashkin MG, Prahl LS, Przybyla LM, McGregor AL, Bell ES, Barnes JM, DuFort CC, Ou G, Chang AC, Cassereau L, Tan SJ, Pickup MW, Lakins JN, Ye X, Davidson MW, Lammerding J, Odde DJ, Dunn AR, Weaver VM (2017) Integrin-mediated traction force enhances paxillin molecular associations and adhesion dynamics that increase the invasiveness of tumor cells into a three-dimensional extracellular matrix. Mol Biol Cell 28(11):1467–1488
49. Callan-Jones AC, Voituriez R (2016) Actin flows in cell migration: from locomotion and polarity to trajectories. Curr Opin Cell Biol 38:12–17
50. Gardel ML, Sabass B, Ji L, Danuser G, Schwarz US, Waterman CM (2008) Traction stress in focal adhesions correlates biphasically with actin retrograde flow speed. J Cell Biol 183(6):999–1005
51. Liu YJ, Le Berre M, Lautenschlaeger F, Maiuri P, Callan-Jones A, Heuzé M, Takaki T, Voituriez R, Piel M (2015) Confinement and low adhesion induce fast amoeboid migration of slow mesenchymal cells. Cell 160(4):659–672
52. Lin CH, Forscher P (1995) Growth cone advance is inversely proportional to retrograde F-actin flow. Neuron 14(4):763–771
53. Hill AV (1938) The heat of shortening and the dynamic constants of muscle. Proc R Soc Lond B Biol Sci 126(843):136–195
54. Cuda G, Pate E, Cooke R, Sellers JR (1997) In vitro actin filament sliding velocities produced by mixtures of different types of myosin. Biophys J 72(4):1767–1779
55. Tsuda Y, Yasutake H, Ishijima A, Yanagida T (1996) Torsional rigidity of single actin filaments and actin-actin bond breaking force under torsion measured directly by in vitro micromanipulation. Proc Natl Acad Sci U S A 93(23):12937–12942
56. Stam S, Alberts J, Gardel ML, Munro E (2015) Isoforms confer characteristic force generation and mechanosensation by myosin II filaments. Biophys J 108(8):1997–2006
57. Sugi H, Chaen S (2003) Force-velocity relationships in actin-myosin interactions causing cytoplasmic streaming in algal cells. J Exp Biol 206(12):1971–1976
58. Barnhart EL, Lee KC, Keren K, Mogilner A, Theriot JA (2011) An adhesion-dependent switch between mechanisms that determine motile cell shape. PLoS Biol 9(5):e1001059
59. Lomakin AJ, Lee KC, Han SJ, Bui DA, Davidson M, Mogilner A, Danuser G (2015) Competition for actin between two distinct F-actin networks defines a bistable switch for cell polarization. Nat Cell Biol 17(11):1435–1445
60. Satulovsky J, Lui R, Wang YL (2008) Exploring the control circuit of cell migration by mathematical modeling. Biophys J 94(9):3671–3683
61. Maiuri P, Rupprecht JF, Wieser S, Ruprecht V, Bénichou O, Carpi N, Coppey M, De Beco S, Gov N, Heisenberg CP, Lage Crespo C, Lautenschlaeger F, Le Berre M, Lennon-Dumenil AM, Raab M, Thiam HR, Piel M, Sixt M, Voituriez R (2015) Actin flows mediate a universal coupling between cell speed and cell persistence. Cell 161(2):374–386

62. Ruprecht V, Wieser S, Callan-Jones A, Smutny M, Morita H, Sako K, Barone V, Ritsch-Marte M, Sixt M, Voituriez R, Heisenberg CP (2015) Cortical contractility triggers a stochastic switch to fast amoeboid cell motility. Cell 160(4):673–685
63. Hawkins RJ, Poincloux R, Bénichou O, Piel M, Chavrier P, Voituriez R (2011) Spontaneous contractility-mediated cortical flow generates cell migration in three-dimensional environments. Biophys J 101(5):1041–1045
64. Campbell ID, Humphries MJ (2011) Integrin structure, activation, and interactions. Cold Spring Harb Perspect Biol 3(3)
65. Ziegler WH, Gingras AR, Critchley DR, Emsley J (2008) Integrin connections to the cytoskeleton through Talin and vinculin. Biochem Soc Trans 36(Pt 2):235–239
66. Gardel ML, Schneider IC, Aratyn-Schaus Y, Waterman CM (2010) Mechanical integration of actin and adhesion dynamics in cell migration. Annu Rev Cell Dev Biol 26:315–333
67. Leckband DE, le Duc Q, Wang N, de Rooij J (2011) Mechanotransduction at cadherin-mediated adhesions. Curr Opin Cell Biol 23(5): 523–530
68. Ponta H, Sherman L, Herrlich PA (2003) CD44: from adhesion molecules to signalling regulators. Nat Rev Mol Cell Biol 4(1):33–45
69. Bell GI (1978) Models for the specific adhesion of cells to cells. Science 200(4342):618–627
70. Oakes PW, Banerjee S, Marchetti MC, Gardel ML (2014) Geometry regulates traction stresses in adherent cells. Biophys J 107(4):825–833
71. Desgrosellier JS, Cheresh DA (2010) Integrins in cancer: biological implications and therapeutic opportunities. Nat Rev Cancer 10(1):9–22
72. Winograd-Katz SE, Fässler R, Geiger B, Legate KR (2014) The integrin adhesome: from genes and proteins to human disease. Nat Rev Mol Cell Biol 15(4):273–288
73. Brown CM, Hebert B, Kolin DL, Zareno J, Whitmore L, Horwitz AR, Wiseman PW (2006) Probing the integrin-actin linkage using high-resolution protein velocity mapping. J Cell Sci 119(Pt 24): 5204–5214
74. Thievessen I, Thompson PM, Berlemont S, Plevock KM, Plotnikov SV, Zemljic-Harpf A, Ross RS, Davidson MW, Danuser G, Campbell SL, Waterman CM (2013) Vinculin-actin interaction couples actin retrograde flow to focal adhesions, but is dispensable for focal adhesion growth. J Cell Biol 202(1):163–177
75. Elosegui-Artola A, Bazellières E, Allen MD, Andreu I, Oria R, Sunyer R, Gomm JJ, Marshall JF, Jones JL, Trepat X, Roca-Cusachs P (2014) Rigidity sensing and adaptation through regulation of integrin types. Nat Mater 13(6):631–637
76. Engler AJ, Sen S, Sweeney HL, Discher DE (2006) Matrix elasticity directs stem cell lineage specification. Cell 126(4):677–689
77. Ulrich TA, de Juan Pardo EM, Kumar S (2009) The mechanical rigidity of the extracellular matrix regulates the structure, motility, and proliferation of glioma cells. Cancer Res 69(10):4167–4174
78. Elosegui-Artola A, Oria R, Chen Y, Kosmalska A, Pérez-González C, Castro N, Zhu C, Trepat X, Roca-Cusachs P (2016) Mechanical regulation of a molecular clutch defines force transmission and transduction in response to matrix rigidity. Nat Cell Biol 18(5):540–548
79. Bangasser BL, Shamsan GA, Chan CE, Opoku KN, Tüzel E, Schlichtmann BW, Kasim JA, Fuller BJ, McCullough BR, Rosenfeld SS, Odde DJ (2017) Shifting the optimal stiffness for cell migration. Nat Commun 8:15313
80. Jiang G, Giannone G, Critchley DR, Fukumoto E, Sheetz MP (2003) Two-piconewton slip bond between fibronectin and the cytoskeleton depends on Talin. Nature 424(6946):334–337
81. Kong F, García AJ, Mould AP, Humphries MJ, Zhu C (2009) Demonstration of catch bonds between an integrin and its ligand. J Cell Biol 185(7): 1275–1284
82. Buckley CD, Tan J, Anderson KL, Hanein D, Volkmann N, Weis WI, Nelson WJ, Dunn AR (2014) Cell adhesion. The minimal cadherin-catenin complex binds to actin filaments under force. Science 346(6209):1254211
83. Pereverzev YV, Prezhdo OV, Forero M, Sokurenko EV, Thomas WE (2005) The two-pathway model for the catch-slip transition in biological adhesion. Biophys J 89(3):1446–1454
84. Yago T, Lou J, Wu T, Yang J, Miner JJ, Coburn L, López JA, Cruz MA, Dong JF, McIntire LV, McEver RP, Zhu C (2008) Platelet glycoprotein Ibalpha forms catch bonds with human WT vWF but not with type 2B von Willebrand disease vWF. J Clin Invest 118(9): 3195–3207
85. Chang AC, Mekhdjian AH, Morimatsu M, Denisin AK, Pruitt BL, Dunn AR (2016) Single molecule force measurements in living cells reveal a minimally tensioned integrin state. ACS Nano 10(12):10745–10752
86. Wang X, Sun J, Xu Q, Chowdhury F, Roein-Peikar M, Wang Y, Ha T (2015) Integrin molecular tension within motile focal adhesions. Biophys J 109(11):2259–2267
87. Li Y, Bhimalapuram P, Dinner AR (2010) Model for how retrograde actin flow regulates adhesion traction stresses. J Phys Condens Matter 22(19):194113
88. Case LB, Waterman CM (2015) Integration of actin dynamics and cell adhesion by a three-dimensional, mechanosensitive molecular clutch. Nat Cell Biol 17(8):955–963

89. Bangasser BL, Rosenfeld SS, Odde DJ (2013) Determinants of maximal force transmission in a motor-clutch model of cell traction in a compliant microenvironment. Biophys J 105(3):581–592
90. Bangasser BL, Odde DJ (2013) Master equation-based analysis of a motor-clutch model for cell traction force. Cell Mol Bioeng 6(4):449–459
91. Plotnikov SV, Pasapera AM, Sabass B, Waterman CM (2012) Force fluctuations within focal adhesions mediate ECM-rigidity sensing to guide directed cell migration. Cell 151(7):1513–1527
92. Chaudhuri O, Gu L, Darnell M, Klumpers D, Bencherif SA, Weaver JC, Huebsch N, Mooney DJ (2015) Substrate stress relaxation regulates cell spreading. Nat Commun 6:6364
93. Weinberg SH, Mair DB, Lemmon CA (2017) Mechanotransduction dynamics at the cell-matrix interface. Biophys J 112(9):1962–1974
94. Hu K, Ji L, Applegate KT, Danuser G, Waterman-Storer CM (2007) Differential transmission of actin motion within focal adhesions. Science 315(5808):111–115
95. Sabass B, Schwarz US (2010) Modeling cytoskeletal flow over adhesion sites: competition between stochastic bond dynamics and intracellular relaxation. J Phys Condens Matter 22(19):194112
96. Welf ES, Johnson HE, Haugh JM (2013) Bidirectional coupling between integrin-mediated signaling and actomyosin mechanics explains matrix-dependent intermittency of leading-edge motility. Mol Biol Cell 24(24):3945–3955
97. Craig EM, Stricker J, Gardel M, Mogilner A (2015) Model for adhesion clutch explains biphasic relationship between actin flow and traction at the cell leading edge. Phys Biol 12(3):035002
98. Webb DJ, Parsons JT, Horwitz AF (2002) Adhesion assembly, disassembly and turnover in migrating cells – over and over and over again. Nat Cell Biol 4(4):E97-100
99. Balaban NQ, Schwarz US, Riveline D, Goichberg P, Tzur G, Sabanay I, Mahalu D, Safran S, Bershadsky A, Addadi L, Geiger B (2001) Force and focal adhesion assembly: a close relationship studied using elastic micropatterned substrates. Nat Cell Biol 3(5):466–472
100. Galbraith CG, Yamada KM, Sheetz MP (2002) The relationship between force and focal complex development. J Cell Biol 159(4):695–705
101. Riveline D, Zamir E, Balaban NQ, Schwarz US, Ishizaki T, Narumiya S, Kam Z, Geiger B, Bershadsky AD (2001) Focal contacts as mechanosensors: externally applied local mechanical force induces growth of focal contacts by an mDia1-dependent and ROCK-independent mechanism. J Cell Biol 153(6):1175–1186
102. Shemesh T, Bershadsky AD, Kozlov MM (2012) Physical model for self-organization of actin cytoskeleton and adhesion complexes at the cell front. Biophys J 102(8):1746–1756
103. Besser A, Safran SA (2006) Force-induced adsorption and anisotropic growth of focal adhesions. Biophys J 90(10):3469–3484
104. Cao X, Lin Y, Driscoll TP, Franco-Barraza J, Cukierman E, Mauck RL, Shenoy VB (2015) A chemomechanical model of matrix and nuclear rigidity regulation of focal adhesion size. Biophys J 109(9):1807–1817
105. Paszek MJ, Zahir N, Johnson KR, Lakins JN, Rozenberg GI, Gefen A, Reinhart-King CA, Margulies SS, Dembo M, Boettiger D, Hammer DA, Weaver VM (2005) Tensional homeostasis and the malignant phenotype. Cancer Cell 8(3): 241–254
106. Wang X, Ha T (2013) Defining single molecular forces required to activate integrin and notch signaling. Science 340(6135):991–994
107. Yao M, Goult BT, Chen H, Cong P, Sheetz MP, Yan J (2014) Mechanical activation of vinculin binding to Talin locks Talin in an unfolded conformation. Sci Rep 4:4610
108. Tozluoğlu M, Tournier AL, Jenkins RP, Hooper S, Bates PA, Sahai E (2013) Matrix geometry determines optimal cancer cell migration strategy and modulates response to interventions. Nat Cell Biol 15(7):751–762
109. Petrie RJ, Koo H, Yamada KM (2014) Generation of compartmentalized pressure by a nuclear piston governs cell motility in a 3D matrix. Science 345(6200):1062–1065
110. Petrie RJ, Harlin HM, Korsak LI, Yamada KM (2017) Activating the nuclear piston mechanism of 3D migration in tumor cells. J Cell Biol 216(1):93–100
111. Manoussaki D, Shin WD, Waterman CM, Chadwick RS (2015) Cytosolic pressure provides a propulsive force comparable to actin polymerization during lamellipod protrusion. Sci Rep 5:12314
112. Davidson PM, Denais C, Bakshi MC, Lammerding J (2014) Nuclear deformability constitutes a rate-limiting step during cell migration in 3-D environments. Cell Mol Bioeng 7(3):293–306
113. Harada T, Swift J, Irianto J, Shin JW, Spinler KR, Athirasala A, Diegmiller R, Dingal PC, Ivanovska IL, Discher DE (2014) Nuclear Lamin stiffness is a barrier to 3D migration, but softness can limit survival. J Cell Biol 204(5):669–682
114. Umeshima H, Hirano T, Kengaku M (2007) Microtubule-based nuclear movement occurs independently of centrosome positioning in migrating neurons. Proc Natl Acad Sci U S A 104(41): 16182–16187
115. Thiam HR, Vargas P, Carpi N, Crespo CL, Raab M, Terriac E, King MC, Jacobelli J, Alberts AS, Stradal T, Lennon-Dumenil AM, Piel M (2016) Perinuclear Arp2/3-driven actin polymerization enables nuclear deformation to facilitate cell migration through complex environments. Nat Commun 7:10997

116. Cao X, Moeendarbary E, Isermann P, Davidson PM, Wang X, Chen MB, Burkart AK, Lammerding J, Kamm RD, Shenoy VB (2016) A chemomechanical model for nuclear morphology and stresses during cell transendothelial migration. Biophys J 111(7):1541–1552
117. Aubry D, Thiam H, Piel M, Allena R (2015) A computational mechanics approach to assess the link between cell morphology and forces during confined migration. Biomech Model Mechanobiol 14(1):143–157
118. Klank RL, Decker Grunke SA, Bangasser BL, Forster CL, Price MA, Odde TJ, SantaCruz KS, Rosenfeld SS, Canoll P, Turley EA, McCarthy JB, Ohlfest JR, Odde DJ (2017) Biphasic dependence of glioma survival and cell migration on CD44 expression level. Cell Rep 18(1):23–31
119. Palecek SP, Loftus JC, Ginsberg MH, Lauffenburger DA, Horwitz AF (1997) Integrin-ligand binding properties govern cell migration speed through cell-substratum adhesiveness. Nature 385(6616):537–540
120. Tranquillo RT, Lauffenburger DA, Zigmond SH (1988) A stochastic model for leukocyte random motility and chemotaxis based on receptor binding fluctuations. J Cell Biol 106(2):303–309
121. Owen LM, Adhikari AS, Patel M, Grimmer P, Leijnse N, Kim MC, Notbohm J, Franck C, Dunn AR (2017) A cytoskeletal clutch mediates cellular force transmission in a soft, three-dimensional extracellular matrix. Mol Biol Cell 28(14):1959–1974
122. Zaman MH, Kamm RD, Matsudaira P, Lauffenburger DA (2005) Computational model for cell migration in three-dimensional matrices. Biophys J 89(2):1389–1397
123. Estabridis HM, Jana A, Nain A, Odde DJ (2018) Cell migration in 1D and 2D nanofiber microenvironments. Ann Biomed Eng 46(3):392–403
124. Ray A, Slama ZM, Morford RK, Madden SA, Provenzano PP (2017) Enhanced directional migration of cancer stem cells in 3D aligned collagen matrices. Biophys J 112(5):1023–1036
125. Zaman MH, Trapani LM, Sieminski AL, Siemeski A, Mackellar D, Gong H, Kamm RD, Wells A, Lauffenburger DA, Matsudaira P (2006) Migration of tumor cells in 3D matrices is governed by matrix stiffness along with cell-matrix adhesion and proteolysis. Proc Natl Acad Sci U S A 103(29):10889–10894
126. Kumar S, Weaver VM (2009) Mechanics, malignancy, and metastasis: the force journey of a tumor cell. Cancer Metastasis Rev 28(1-2):113–127
127. Peyton SR, Putnam AJ (2005) Extracellular matrix rigidity governs smooth muscle cell motility in a biphasic fashion. J Cell Physiol 204(1):198–209
128. Stroka KM, Aranda-Espinoza H (2009) Neutrophils display biphasic relationship between migration and substrate stiffness. Cell Motil Cytoskeleton 66(6):328–341
129. Lo CM, Wang HB, Dembo M, Wang YL (2000) Cell movement is guided by the rigidity of the substrate. Biophys J 79(1):144–152
130. Gillespie DT (1977) Exact stochastic simulation of coupled chemical reactions. J Phys Chem 81(25):2340–2361
131. Acerbi I, Cassereau L, Dean I, Shi Q, Au A, Park C, Chen YY, Liphardt J, Hwang ES, Weaver VM (2015) Human breast cancer invasion and aggression correlates with ECM stiffening and immune cell infiltration. Integr Biol 7(10):1120–1134
132. Morimatsu M, Mekhdjian AH, Adhikari AS, Dunn AR (2013) Molecular tension sensors report forces generated by single integrin molecules in living cells. Nano Lett 13(9):3985–3989
133. Kanteti R, Batra SK, Lennon FE, Salgia R (2016) FAK and paxillin, two potential targets in pancreatic cancer. Oncotarget 7(21):31586–31601
134. Novak U, Kaye AH (2000) Extracellular matrix and the brain: components and function. J Clin Neurosci 7(4):280–290
135. Bhat KP, Balasubramaniyan V, Vaillant B, Ezhilarasan R, Hummelink K, Hollingsworth F, Wani K, Heathcock L, James JD, Goodman LD, Conroy S, Long L, Lelic N, Wang S, Gumin J, Raj D, Kodama Y, Raghunathan A, Olar A, Joshi K, Pelloski CE, Heimberger A, Kim SH, Cahill DP, Rao G, Den Dunnen WF, Boddeke HW, Phillips HS, Nakano I, Lang FF, Colman H, Sulman EP, Aldape K (2013) Mesenchymal differentiation mediated by NF-κB promotes radiation resistance in glioblastoma. Cancer Cell 24(3):331–346
136. Wei KC, Huang CY, Chen PY, Feng LY, Wu TW, Chen SM, Tsai HC, Lu YJ, Tsang NM, Tseng CK, Pai PC, Shin JW (2010) Evaluation of the prognostic value of CD44 in glioblastoma multiforme. Anticancer Res 30(1):253–259
137. Ranuncolo SM, Ladeda V, Specterman S, Varela M, Lastiri J, Morandi A, Matos E, Bal de Kier Joffé E, Puricelli L, Pallotta MG (2002) CD44 expression in human gliomas. J Surg Oncol 79(1):30–35; discussion 35-6
138. Levin EG (2005) Cancer therapy through control of cell migration. Curr Cancer Drug Targets 5(7):505–518
139. Palmer TD, Ashby WJ, Lewis JD, Zijlstra A (2011) Targeting tumor cell motility to prevent metastasis. Adv Drug Deliv Rev 63(8):568–581
140. Marelli UK, Rechenmacher F, Sobahi TR, Mas-Moruno C, Kessler H (2013) Tumor targeting via integrin ligands. Front Oncol 3:222
141. Mas-Moruno C, Rechenmacher F, Kessler H (2010) Cilengitide: the first anti-angiogenic small molecule drug candidate design, synthesis and clinical evaluation. Anti Cancer Agents Med Chem 10(10):753–768
142. Baker AM, Bird D, Lang G, Cox TR, Erler JT (2013) Lysyl oxidase enzymatic function increases stiffness to drive colorectal can-

cer progression through FAK. Oncogene 32(14): 1863–1868
143. Berg WA, Madsen KS, Schilling K, Tartar M, Pisano ED, Larsen LH, Narayanan D, Kalinyak JE (2012) Comparative effectiveness of positron emission mammography and MRI in the contralateral breast of women with newly diagnosed breast cancer. ARJ Am J Roentgenol 198(1): 219–232
144. Hayashi M, Yamamoto Y, Sueta A, Tomiguchi M, Yamamoto-Ibusuki M, Kawasoe T, Hamada A, Iwase H (2015) Associations between elastography findings and clinicopathological factors in breast cancer. Medicine 94(50):e2290
145. Miroshnikova YA, Mouw JK, Barnes JM, Pickup MW, Lakins JN, Kim Y, Lobo K, Persson AI, Reis GF, McKnight TR, Holland EC, Phillips JJ, Weaver VM (2016) Tissue mechanics promote IDH1-dependent HIF1α-tenascin C feedback to regulate glioblastoma aggression. Nat Cell Biol 18(12):1336–1345
146. Samuel MS, Lopez JI, McGhee EJ, Croft DR, Strachan D, Timpson P, Munro J, Schröder E, Zhou J, Brunton VG, Barker N, Clevers H,Sansom OJ, Anderson KI, Weaver VM, Olson MF (2011) Actomyosin-mediated cellular tension drives increased tissue stiffness and β-catenin activation to induce epidermal hyperplasia and tumor growth. Cancer Cell 19(6):776–791
147. Borghi N, Sorokina M, Shcherbakova OG, Weis WI, Pruitt BL, Nelson WJ, Dunn AR (2012) E-cadherin is under constitutive actomyosin-generated tension that is increased at cell-cell contacts upon externally applied stretch. Proc Natl Acad Sci U S A 109(31):12568–12573
148. Angelini TE, Hannezo E, Trepat X, Marquez M, Fredberg JJ, Weitz DA (2011) Glass-like dynamics of collective cell migration. Proc Natl Acad Sci U S A 108(12):4714–4719
149. Garcia S, Hannezo E, Elgeti J, Joanny JF, Silberzan P, Gov NS (2015) Physics of active jamming during collective cellular motion in a monolayer. Proc Natl Acad Sci U S A 112(50):15314–15319
150. Sunyer R, Conte V, Escribano J, Elosegui-Artola A, Labernadie A, Valon L, Navajas D, García-Aznar JM, Muñoz JJ, Roca-Cusachs P, Trepat X (2016) Collective cell durotaxis emerges from long-range intercellular force transmission. Science 353(6304):1157–1161